

 Open access • Posted Content • DOI:10.1101/804443

Deep metagenomics examines the oral microbiome during dental caries, revealing novel taxa and co-occurrences with host molecules — [Source link](#)

Jonathon L. Baker, James T. Morton, Márcia Dinis, R. Alvarez ...+3 more authors

Institutions: J. Craig Venter Institute, University of California, Los Angeles

Published on: 15 Oct 2019 - bioRxiv (Cold Spring Harbor Laboratory)

Topics: Oral Microbiome and Metagenomics

Related papers:

- [Saliva microbiomes distinguish caries-active from healthy human populations](#)
- [The Dental Plaque Microbiome in Health and Disease](#)
- [Exploration of Human Salivary Microbiomes—Insights into the Novel Characteristics of Microbial Community Structure in Caries and Caries-Free Subjects](#)
- [Oral Microbiome Alterations Associated with Early Childhood Caries Highlight the Importance of Carbohydrate Metabolic Activities.](#)
- [Metagenome sequencing-based strain-level and functional characterization of supragingival microbiome associated with dental caries in children.](#)

Share this paper:    

View more about this paper here: <https://typeset.io/papers/deep-metagenomics-examines-the-oral-microbiome-during-dental-3no2pqdt5g>

1 **Working Title: Deep metagenomics examines the oral microbiome during dental caries,**
2 **revealing novel taxa and co-occurrences with host molecules**

3
4 **Authors: Baker, J.L.^{1,*}, Morton, J.T.², Dinis, M.³, Alvarez, R.³, Tran, N.C.³, Knight, R.^{4,5,6,7},**
5 **Edlund, A.^{1,*}**

6 ¹ Genomic Medicine Group
7 J. Craig Venter Institute
8 4120 Capricorn Ln.
9 La Jolla, CA 92037

10
11 ²Systems Biology Group
12 Flatiron Institute
13 162 5th Avenue
14 New York, NY 10010

15
16 ³Section of Pediatric Dentistry
17 UCLA School of Dentistry
18 10833 Le Conte Ave.
19 Los Angeles, CA 90095-1668

20
21 ⁴Department of Computer Science and Engineering
22 University of California at San Diego
23 9500 Gilman Drive
24 La Jolla, CA 92093

25
26 ⁵Center for Microbiome Innovation
27 University of California at San Diego
28 La Jolla, CA 92023

29
30 ⁶Department of Pediatrics
31 University of California at San Diego
32 La Jolla, CA 92023

33
34 ⁷Department of Bioengineering
35 University of California at San Diego
36 9500 Gilman Drive
37 La Jolla, CA 92093

38
39
40 *Corresponding Authors: JLB: jobaker@jcvl.org, AE: aedlund@jcvl.org

41
42 ORCIDs: JLB: 0000-0001-5378-322X

43
44

45 **Abstract**

46 Dental caries is the most common chronic infectious disease globally. The microbial communities
47 associated with caries have mainly been examined using relatively low-resolution 16S rRNA gene
48 amplicon sequencing and/or using downstream analyses that are unsound for the compositional
49 nature of the data provided by sequencing. Additionally, the relationship between caries, oral
50 microbiome composition, and host immunological markers has not been explored. In this study,
51 the oral microbiome and a panel of 38 host markers was analyzed across the saliva from 23
52 children with dentin caries and 24 children with healthy dentition. Metagenomic sequencing,
53 followed by investigation using tools designed to be robust for compositional data, illustrated
54 that several *Prevotella* spp. were prevalent in caries, while *Rothia* spp. were associated with the
55 health. The contributinal diversity (extent to which multiple taxa contribute to each pathway)
56 of functional pathways present in the oral microbiome was decreased in the caries group. This
57 decrease was especially noticeable in several pathways known to impede caries pathogenesis,
58 including arginine and branched-chain amino acid biosynthesis. 10 host immunological markers
59 were found to be significantly elevated in the saliva of the caries group, and microbe-metabolite
60 co-occurrence analysis provided an atlas of relationships contributing to the bi-directional
61 influence between the oral microbiome and the host immune system. Finally, 527 metagenome-
62 assembled genomes were obtained from the metagenomics data, representing 151 species. 23
63 taxa were novel genera/species and a further 20 taxa were novel species. This study thus serves
64 as a model analysis pipeline that will tremendously expand our knowledge of the oral microbiome
65 and its relationship to dental caries once applied to large populations.

66

67 **Introduction**

68 Dental caries is the most common chronic infectious disease and will afflict well over half of the
69 global human population at some point in their lives. Dental caries is particularly problematic in
70 children, where it is five times more common than asthma, the second most common chronic
71 disease. This extreme prevalence translates to an extraordinary economic burden. Caries
72 disproportionately afflicts vulnerable populations least able to access and afford proper treatment
73 (1). Historically, members of the acid-producing and acid-tolerant mutans group of streptococci,
74 particularly the paradigm species of the group, *Streptococcus mutans*, were considered the
75 etiologic agents of the disease (2). While caries is certainly an infectious and transmissible
76 disease caused by the oral microbiota, it is now understood to be multifactorial and ecology-
77 based, because although mutans streptococci are commonly associated with caries, they are
78 neither necessary nor sufficient to cause disease (3). Interplay between host genetic and
79 immunological factors, diet and hygiene habits, and the oral microbiota affect clinical development
80 of the disease (1, 4).

81 Second-generation sequencing techniques enabled many studies characterizing the oral
82 microbiome to distinguish healthy individuals from those with dental caries. The highlights and
83 challenges of this progress have been the subject of several excellent recent reviews (5-7). These
84 studies of the oral microbiome in the context of dental caries have yielded varied results,
85 particularly vis-à-vis the association (and therefore inferred importance) of *S. mutans* and other
86 taxa with the disease. This has rightfully led to some debate regarding the long-standing dogma
87 that *S. mutans* is a keystone species in caries pathogenesis (3, 8, 9). These studies used widely
88 different sampling techniques, library prep methods, and data analysis methods, which contribute
89 substantially to variation among studies. Furthermore, ethnicity, immunology, diet, hygiene and
90 other factors also likely contribute variability and are difficult to control. Finally, because
91 microbiome sequencing provides data in the form of relative abundances, inferring absolute fold-
92 changes or correlations is inherently problematic (10-13). Numerous microbiome studies have

93 drawn biological conclusions based on the application of conventional statistical tools to
94 compositional data, which has been shown to have unacceptably high false discovery rates and
95 lead to spurious hypotheses (11).

96 The overwhelming majority of studies examining the microbiome associated with caries
97 have utilized 16S rRNA gene amplicon sequencing (“16S sequencing”) (9). While 16S
98 sequencing is widely used, relatively inexpensive, and has significantly advanced the field of
99 microbiology, there are a number of disadvantages to using this technique. These include the
100 biases introduced during the PCR amplification step (i.e. different 16S amplicons amplify at
101 different efficiencies for various species and genera), biases due to the fact that many taxa encode
102 differing copy numbers of the 16S gene, and the inability to distinguish organisms at the strain,
103 species, or, occasionally, even higher taxonomic level (14-17). For example, *S. mutans*, an
104 overtly cariogenic species, and *Streptococcus gordonii*, largely associated with good dental
105 health, are both simply identified as ‘*Streptococcus*’ in many 16S-based studies. In addition,
106 studies have suggested that compositional differences at the species level can, at times, be less
107 reflective of the health of a microbial community than differences in the metabolic functions of the
108 community (i.e. interpersonal microbial taxonomic profiles may be significantly different, but
109 communities remain more or less functionally equivalent) (18). Although bioinformatics tools,
110 such as PICRUSt (19), predict community functions based on 16S amplicon sequencing,
111 evidence continues to mount that the pan-genomic (i.e. intra-species) diversity of many individual
112 taxa is massive, limiting the utility of such predictions when the key genes involved in a biological
113 process are not conserved phylogenetically or among strains of a species. In the case of dental
114 caries, this strain-to-strain variation is well-documented to affect both virulence of pathogens (e.g.
115 *S. mutans*) and protective effects of commensals (e.g. *S. gordonii*), further illustrating a need for
116 studies utilizing more in-depth sequencing and analysis methods (5). Although several shotgun
117 metagenomic surveys of the oral microbiota have been performed (20-23), they have not

118 employed differential ranking techniques with consistent reference frames, as detailed in Morton
119 et al. 2019 (13).

120 In this study, shotgun metagenomic sequencing was used to examine the oral microbiome
121 of 23 children with severe dentin caries, compared to 24 children with good dental health. The
122 study groups were not equal numbers due to difficulties in recruitment. This shotgun sequencing,
123 followed by investigation using state-of-the-art tools for analysis of compositional data and
124 generation of metagenome-assembled genomes (MAGs), allowed identification and relative
125 quantification of species and strain-level taxa, analysis of the functional pathways present, and
126 reconstruction of high-quality species-level genomes, including those of nearly 50 novel taxa.

127 The oral samples utilized for metagenomic sequencing were also tested for the presence
128 of 38 salivary immunological markers, 10 of which were significantly elevated in the caries group.
129 Although dental caries pathogenesis originates on the non-shedding, hard surface of the tooth,
130 the immunology of the human host nevertheless plays a critical role in disease prevention or
131 progression. Both the innate and adaptive arms of the immune system influence caries, and past
132 proof-of-principle studies explored the possibility of several active and passive vaccine strategies
133 to prevent caries (reviewed in (24, 25)). In recent years, however, research regarding the
134 immunological component of dental caries has lagged well behind study of the microbiological
135 component. This is due at least in part to the prevailing perception of dental caries as an ‘over-
136 the-counter’ disease (26). The oral microbiota clearly influences the host immune system and
137 vice-versa, and it is likely that in cases of good oral health, the immune system has evolved to
138 tolerate and facilitate maintenance of a commensal, yet territorial oral microbiota that prevents
139 the establishment of foreign pathogens (27). The co-occurrence analysis performed in this study
140 between microbial features and salivary immunological markers provides the first detailed look at
141 potential cross-talk between the oral microbiota and the immune system of the human host during
142 advanced dental caries compared to health.

143

144 **RESULTS**

145

146 **Study design (Figure 1A).** Details of the clinical sampling, as well as inclusion and exclusion
147 criteria are provided in the MATERIALS AND METHODS section. In brief, 47 participants aged 4-11
148 received a comprehensive oral examination, and their dental caries status was recorded using
149 decayed (d), missing due to decay (m), or filled (f) teeth in primary and permanent dentitions
150 (dmft/DMFT) by a clinician (Fig 1A). A summary of the collected subject metadata is provided in
151 Table S1. Subjects were dichotomized into two groups: healthy (0 decayed, missing, or filled
152 teeth [DMFT]), or caries (≥ 2 active caries lesions with penetration through the enamel into the
153 underlying dentin, only lesions at least 2 mm in depth were considered). All subjects provided 2
154 ml of unstimulated saliva and 2ml of stimulated saliva, which was clarified by centrifugation. DNA
155 was extracted from the stimulated saliva samples and subjected to Illumina sequencing and
156 metagenomics analysis as described in MATERIALS AND METHODS. The concentration of 38
157 immunological markers in the unstimulated saliva samples were determined using a multiplex
158 Luminex bead immunoassay performed by Westcoast Biosciences. Dataset S1 contains the
159 comprehensive output of the Luminex assay. A detailed summary of the bioinformatics tools and
160 pipelines used in this study are provided in Figure 1B.

161

162 **In this study group, *Prevotella* spp. were associated with disease, while *Rothia* spp. were**
163 **associated with good dental health.** Following quality control performed by KneadData
164 (available at <https://bitbucket.org/biobakery/kneaddata>), MetaPhlan2 (28) was utilized to
165 determine the relative abundance of microbial taxa within each sample. The most abundant taxa
166 across all samples belonged to the taxonomic groups *Prevotella*, *Veillonella*, *Porphyromonas*,
167 *Rothia*, *Haemophilus*, *Streptococcus*, and *Saccharibacteria* (Figure 2A and S1). Notable trends
168 included a higher relative abundance of *Rothia* spp., *Porphyromonas* sp. oral taxon 270,
169 *Haemophilus parainfluenzae* and *Streptococcus sanguinis* in the saliva from healthy children

170 (Figure 2A). Meanwhile, although *S. mutans* was detected at higher relative abundances in the
171 saliva derived from the children with caries, *S. mutans* and the other canonical caries pathogen,
172 *Streptococcus sobrinus*, were observed in comparably low relative abundances overall, and only
173 within 11 and 3 samples, respectively (*S. mutans*: 7 caries and 4 healthy; *S. sobrinus*: 2 caries, 1
174 healthy). The complete taxonomic table generated by MetaPhlan2 is provided in Table S2 and a
175 heatmap is provided in Figure S1.

176 Alpha diversity (within-sample diversity), was calculated using QIIME2 (29), was not
177 significantly different between the healthy and caries groups, and was not correlated to DMFT
178 scores, Age, Lesion Depth, or the Number of Lesions, according to the Shannon and Simpson
179 metrics (data not shown). Beta diversity (between sample diversity) was determined using
180 DEICODE (30), which utilizes matrix completion and robust Aitchison principal component
181 analysis (RPCA), providing several advantages over other tools, including the ability to accurately
182 handle sparse datasets (e.g. in most microbial communities, most taxa are not present in a
183 majority of samples), scale invariance (negating the need for rarefaction) and preservation of
184 feature loadings (facilitating the analysis of which taxa are driving the differences in the ordination
185 space)(30). DEICODE illustrated a clear difference in beta diversity between the healthy and
186 caries subject groups (Figure 2B), which was statistically significant based upon a PERMANOVA
187 ($p = 0.003$), and occurred mainly along Axis 2 (the vertical axis). The 15 species that were the
188 most significant drivers of distance in ordination space are illustrated by the vectors in Figure 2B.
189 Qurro (doi:10.5281/zenodo.3369454) was used to visualize and identify taxa driving the
190 differences along Axis 2, which seemed to correspond to separation between the healthy and
191 caries samples in the ordination space (Figure 2C). *Prevotella histicola*, *Prevotella salivae*, and
192 *Prevotella pallens* were the top 3 drivers in the positive direction along Axis 2 (corresponding to
193 the caries samples), while *Rothia mucilaginosa* and *Rothia aerea* were the top 2 drivers in the
194 negative direction along Axis 2 (corresponding to the healthy samples) (Figure 2C). Certain
195 *Neisseria* and *Haemophilus* spp. also seemed to be generally associated with the healthy

196 samples (Figure 2B and C). *S. mutans*, the classic caries pathogen, did not appear to be a major
197 driver of beta diversity, according to DEICODE (Figure 2C).

198

199 **Differential ranking reveals *S. mutans* is significantly associated with caries.** As the
200 patterns observed above used taxa ranked in an unsupervised manner, it was important to
201 determine which taxa were directly associated with disease status (and not simply Axis 2 of the
202 DEICODE biplot). Songbird (13) and Qurro were used to respectively calculate and display the
203 differential ranks of taxa directly associated with health versus disease (Figure 2D). Because this
204 method is sensitive to sparsity, only species observed in at least 10 samples and having over
205 10,000 total predicted counts were analyzed here. A similar pattern was observed using this
206 approach, with several *Prevotella* species the most correlated taxa the caries samples and all 3
207 observed *Rothia* species correlated with the health samples, as were most *Neisseria* and
208 *Haemophilus* spp. (Figure 2D). Differential ranks are listed in Table S3. Interestingly, *S. mutans*,
209 the classic caries pathogen, was the third-highest-ranked taxon in association with the caries
210 samples (Figure 2D). Log ratios are a preferable way to examine differences within compositional
211 datasets (13), and as *Prevotella* spp. were significantly associated with the caries samples and
212 *Rothia*, *Haemophilus* and *Neisseria* spp. were strongly associated with the healthy samples,
213 according to both unsupervised and supervised methods, the log ratios of *Prevotella* to *Rothia*,
214 *Haemophilus* and *Neisseria* were examined. In all three cases, the log-ratio with *Prevotella* as
215 the numerator was significantly higher in the caries group compared to the healthy group,
216 indicating that the ratio of these taxa may have clinical significance and be a useful marker of
217 disease (Figure 2E). Although the ranking of *Prevotella*, *Rothia*, *Haemophilus*, and *Neisseria* in
218 regards to disease status is generally concordant between DEICODE and Songbird, there is some
219 discrepancy in the ranks of other taxa, mainly low-abundance. This is likely due the nature of
220 multinomial regression (employed by Songbird), in which features with low counts can have a
221 larger fold change than features with high counts. *Rothia* is a genus that has received little

222 attention and has been previously associated with either caries or good dental health, depending
223 on the study (possibly due to use of non-compositional data analyses), indicating that this taxon
224 demands further examination (13, 31, 32).

225

226 **Fungi and viruses are present in low numbers in the oral microbiomes examined in this**

227 **study.** Unlike 16S sequencing, metagenomic sequencing detects viruses and eukaryotes in

228 addition to bacteria. 12 viruses were detected in this study, including several human

229 herpesviruses and several bacteriophage (Figure 2A). The viruses were detected at relatively

230 low frequency and did not appear to be significant drivers of beta diversity in this study group

231 (Figure 2). The fungal pathogen, *Candida albicans* is known to be involved in pathogenesis in

232 many cases of dental caries (reviewed in (33)), therefore it was surprising that it was not detected

233 by MetaPhlan2 in this study. Mapping Illumina reads directly to the *C. albicans* genome indicated

234 the presence of *C. albicans* in the samples, but the number of reads was small, and thus any

235 fungal pathogens present in the study group were likely to be below the threshold of detection

236 employed in taxonomic quantification by MetaPhlan2 (data not shown). It is possible that the

237 extraction methods used did not efficiently lyse fungal cells, leading to an observed

238 underrepresentation.

239

240 **There is a decrease in the diversity of functional pathways in the oral microbiome of**

241 **children with caries.** To examine the differential representation of particular microbial metabolic

242 and biosynthetic pathways in caries and health, HUMAnN2 (34) analysis was performed on the

243 quality-controlled Illumina reads. The resulting pathway abundance table (Table S4, Figure S2)

244 was analyzed using QIIME2, DEICODE, and Songbird. The functional pathways of the oral

245 microbiome from the caries group had a lower alpha diversity, as measured using the Shannon

246 Index (Figure 3A), and this metric inversely correlated with the number of lesions (Figure S3).

247 99.97% of the functional pathway beta diversity was explained by one PCA axis in the DEICODE

248 biplot (Figure 3B), and disease status was less associated with functional than taxonomic pathway
249 beta diversity (PERMANOVA, $P = 0.016$ vs 0.003). This reduction in variance made it difficult to
250 interpret whether any pathways were correlated to disease status. Rare, low abundance features
251 were most strongly associated with the caries group, while several pathways, including anaerobic
252 and aerobic energy metabolism, were associated with health as shown in results from DEICODE
253 (Figure 3B) and Songbird (Table S5). One of the advantages of HUMAnN2 is the ability to stratify
254 pathways by taxa and examine contributonal diversity, the extent to which multiple taxa contribute
255 to particular functional pathway (34). Across the 69 core functional pathways which were present
256 in all 47 samples and had more than 3 contributing taxa, contributonal diversity was decreased
257 in the caries group compared to the healthy group (Figure 3C). This was more noticeable along
258 the x-axis, corresponding to alpha diversity, and congruent with the data provided in Figures 3A
259 and B, which was agnostic to contributing taxa. Contributonal diversity was examined for several
260 specific pathways identified as health-associated in Songbird, and several pathways that have a
261 well-established connection to the prevention of caries pathogenesis, including arginine
262 biosynthesis (35), unsaturated fatty acid biosynthesis (36), branched-chain amino acid (BCAA)
263 biosynthesis (37), and urea metabolism (38). The differences seen in several of these pathways
264 were particularly striking (Figures 3D-H). Overall, the data from the functional analyses of the
265 oral microbiome indicates that there is less variation between caries and health in terms of
266 functional pathways compared to taxa. However, several pathways were clearly associated with
267 the healthy samples, including several where the physiological relationship to caries pathogenesis
268 is understood.

269
270 **10 host salivary immunological markers are more abundant in the saliva of children with**
271 **caries than children with good dental health, and co-occur with *Prevotella histicola*,**
272 ***Prevotella salivae*, and *Veilonella atypica*.** To investigate differences in the oral immunological
273 profile of healthy children compared to children with caries, a Luminex bead assay was used to

274 quantify 38 known immunological markers. Of these 38 molecules, 7 were at undetectable levels
275 in >50% of the samples (the columns on the far right of Table S1, with a grey background), and
276 thus were not analyzed further. Based on a Welch's t-test, 10 of the remaining salivary
277 immunological markers were found at significantly higher concentrations in the saliva of children
278 with caries. These were: epidermal growth factor (EGF), interleukin-10 (IL-10), granulocyte-
279 colony stimulating factor (G-CSF), interleukin-1 receptor agonist (IL1-RA),
280 granulocyte/macrophage-colony stimulating factor (GM-CSF), macrophage-derived chemokine
281 (MDC), interleukin-13 (IL-13), interleukin-15 (IL-15), and interleukin-6 (IL-6) (Figure 4A-J). None
282 of the immunological markers were significantly correlated with alpha diversity of the taxa or
283 functional pathways within the samples (data not shown). To examine co-occurrences between
284 specific bacterial species and immunological markers, MMvec
285 (<https://github.com/biocore/mmvec>) was used to create microbe-metabolite vectors, which were
286 visualized using the QIIME2 Emperor plugin (39). Interestingly, there was a noticeable separation
287 of the directionality of several vectors representing taxa associated with caries (e.g. *Prevotella*
288 *histicola*, *Prevotella salivae*, and *Veillonella atypica*) (Figure 4K). These vectors indicated co-
289 occurrence with EGF, IL-10, and IL-1RA (Figure 4K). *Rothia mucilaginosa*, *Haemophilus*
290 *parainfluenzae*, *Streptococcus australis*, and unclassified *Neisseria* formed a cluster of health-
291 associated vectors, and displayed co-occurrence with MCP3 and VEGF (Figure 4K). GRO, MIP-
292 1b, IP-10, MIP-1a, and IL_8 did not appear to have a high co-occurrence with any taxa (Figure
293 4K). Interestingly, although Streptococcal species did not appear to be large drivers of beta
294 diversity (Figure 2B), a number of Streptococcus species did have considerable co-occurrence
295 with host immunological markers (Figure 4K). A similar approach was attempted to examine co-
296 occurrences between functional pathways and the host markers, but MMvec was developed for
297 taxa-metabolite co-occurrences, and the low dimensionality of the functional pathway data made
298 interpreting the results difficult (Figure S4).

299

300 **Assembly of metagenome assembled genomes (MAGs) recovers 527 medium and high-**
301 **quality genomes, 20 representing novel species and 23 representing novel genera and**
302 **species.** A more detailed description of the MAG recovery and results is provided in
303 Supplemental Note 1. The metagenomics pipeline illustrated in Figure 1B yielded 527 bins that
304 were of at least Medium Quality according to the guidelines set forth by the Genomic Standards
305 Consortium (GSC) regarding the Minimum Information about a Metagenome-Assembled Genome
306 (MIMAG) (>50% completeness, <10% contamination) (Table S6) (40). A separate assembly was
307 performed for each sample, as opposed to a co-assembly of all samples, an alternative approach
308 used by some studies. The pros and cons of a co-assembly versus individual assemblies have
309 been discussed previously (41). As a result of the individual assemblies, many of the 527 MAGs
310 were likely to represent redundant species across samples. Following dereplication using fastANI
311 (42) and taxonomic assignment using Mash (43), there were 95 known species level genome bins
312 (kSGBs), representing 376 MAGs and 56 unknown SGBs (uSGBs), representing 126 MAGs
313 (Figure 5A). Further examination of the uSGBs reassigned 15 uSGBs, representing 30 MAGs, to
314 kSGBs, as they had >95% ANI match in GenBank (Table S7). 20 uSGBs, representing 50 MAGs,
315 that had 85%-95% ANI match to a GenBank genome were termed genus-level genome bins
316 (GGBs), as the genus can be assigned with a fair amount of confidence, while the species
317 appears to be not previously described. 23 bins, representing 48 MAGs had no match reference
318 in GenBank with an ANI >85%. These were termed family-level genome bins (FGBs), as the
319 family or higher-level taxa can be inferred, but the MAGs likely represent novel genera. Although
320 the GGBs and FGBs on average had lower completion and higher contamination than the SGBs,
321 all MAGs met the MIMAG standard for medium quality genomes (40) and the FGBs actually had
322 a higher completeness and lower contigs/Mbp than GGBs (Figure 5B-E).

323 PhyloPhlAn2 (41) was used to phylogenetically place the uSGBs amongst reference
324 strains at the order or class level. 25 of the MAGs, including 6 GGB and 11 FGB, appeared to be
325 Candidate Phyla Radiation (CPR) bacteria. This recently described supergroup is predicted to

326 contain >35 phyla representing >15% of the diversity of all bacteria (44). CPR taxa have long
327 been considered microbial “dark matter” and only one species has been cultivated thus far (45).
328 CPR have reduced genomes and are thought to be obligate epibionts (46). In this MAGs dataset,
329 22 CPR MAGs were Saccharibacteria (formerly known as TM7), while 2 CPR MAGs were
330 Gracilibacteria and one was an Absconditabacteria (formerly known as SR1). A comprehensive
331 phylogeny of currently available Saccharibacteria was recently reported, and novel named
332 taxonomic hierarchies proposed (47). In the present study, the Saccharibacteria MAGs represent
333 Groups 1 (order Nanosynbacteriaceae), 3 (order Nanosynsoccalia), and 6 (order
334 Nanoperiomorables). A table with information regarding the CPR MAGs reported here is provided
335 in Table S9 and the phylogenetic trees are provided in Figure 4F (for Saccharibacteria) and Figure
336 S5.

337 GGBs other than the CPR included novel species within the genera *Peptostreptococcus*,
338 *Solobacterium*, *Streptococcus*, *Lachnospiraceae*, *Campylobacter*, *Atopobium*, *Fusobacterium*,
339 *Thermononospora*, *Schaalia*, *Parvimonas*, *Riemerella*, and *Granulicatella*. The
340 *Peptostreptococcus* and two *Solobaceterium* GGBs were particularly interesting as they
341 contained 8, 22, and 3 MAGs, respectively, indicating that these novel species may be somewhat
342 widespread in the study population. FGBs represented novel genera and species within the
343 taxonomic groups Atopobiaceae, Bacteroidales, Campylobacteriaceae, Clostridiales,
344 Lachnospiraceae, Porphyromonadaceae, and Prevotellaceae. Details regarding the GGBs and
345 FGBs are provided in Tables S10 and S11, respectively. Many of the non-CPR uSGBs were
346 found in the clades Bacteroidales and Clostridiales, and phylogenetic trees illustrating uSGB
347 placement within these groups is provided in Figures 5G, 5H, S6, and S7.

348 The final set of MAGs was uploaded to the PATRIC database for annotation and curation
349 using the PATRIC CLI (48), and are publicly available in the PATRIC database and RefSeq. (will
350 be made live/public following acceptance for publication) iRep (49) was used to calculate the

351 replication rates of MAGs, but no difference in replication rates was detected between caries and

352 health (Figure S9, Supplemental Note 2)

353

354 **DISCUSSION**

355

356 Dental caries has been known to be of bacterial origin for many decades. However, due to the
357 “Great Plate Count Anomaly”, the true complexity of the oral microbiota (and that of indeed every
358 microbiota!) has only begun to be realized following the relatively recent development of culture-
359 independent detection methods, such as second-generation sequencing technologies (5, 9, 16,
360 50). Of these techniques, 16S sequencing has been the most widely utilized technique in
361 characterizing microbial communities, including those of the oral cavity associated with dental
362 caries. However, 16S sequencing provides relatively low-resolution data that is biased, due to
363 the PCR amplification step, and overlooks crucial information regarding the true diversity and
364 functional capabilities of the communities present (14-16, 51). Sequencing is also used to
365 quantify the resident taxa in microbial communities. However, sequencing provides only
366 compositional data, which must be handled carefully to avoid generating spurious conclusions—
367 a fact that is frequently swept under the rug by microbiome studies (10-13). Meanwhile, several
368 recent landmark metagenomics studies, focused on the gut microbiome, have provided excellent
369 examples of analyzing metagenomic (i.e. shotgun, whole genome sequencing) datasets,
370 assembling quality MAGs, and have discovered a vast diversity of novel taxa (41, 52, 53). Major
371 goals of this study were to perform relatively deep metagenomic sequencing to observe the
372 microbiome present in the saliva of healthy children compared to the saliva of children with
373 multiple dentin caries, and possibly identify novel taxa. The choice to sample saliva was mainly
374 due to the ease of collection and ability to obtain sufficient sample volume for analysis (particularly
375 for the case of the host markers). While the various microenvironments of the oral cavity have
376 highly distinct microbial residents, and an ideal sampling scenario would examine diversity on this
377 scale, saliva bathes all oral tissues and is generally thought to represent the overall oral
378 composition (7). Differing sampling methods are likely to account for a sizable portion of the
379 variability seen across oral microbiome studies regarding dental caries (7). Another goal of this

380 study was to examine the concentration of host immunological markers present in saliva in caries
381 versus health, and identify microbe-metabolite co-occurrences using a recently developed
382 machine-learning-based tool to examine such relationships in compositional data
383 (<https://github.com/biocore/mmvec>). This cross-talk between the oral microbiome and host
384 molecules in dental caries, compared to health, is not well characterized.

385 This study examined the saliva of 47 children, 4-11 years old. Twenty-four children had
386 good dental health, while 23 children had at least two carious lesions that had penetrated the
387 enamel into the underlying dentin (≥ 2 mm deep dentin lesions), representing a relatively advanced
388 disease state (1). Beta diversity of species-level taxonomy was significantly different between
389 the caries and healthy groups. Notably, the canonical cariogenic species, *S. mutans*, was
390 significantly associated with caries (3rd most correlated species-level taxa according to supervised
391 methods), but was found in relatively low abundances, and in only 11 of the 47 subjects. This
392 indicates that *S. mutans*, when present, has a large influence on the pathogenicity of the oral
393 microbiome due to its prodigious capacity to generate insoluble glucans and resultant biofilms (9,
394 26). Other oral microbiome studies have found *S. mutans* at low abundances (20, 21, 54), and
395 the use of saliva in this study may explain its rarity, and possibly underestimation, here—as an
396 exceptional biofilm-former, it is less likely to be shed from its dental plaque residence into the
397 salivary milieu (55).

398 Both unsupervised and supervised methods showed that *Rothia*, *Neisseria* and
399 *Haemophilus* spp. were associated with health, and several abundant *Prevotella* spp. (*P. histicola*,
400 *P. pallens*, and *P. salivae*) were associated with disease. Although *Prevotella* spp. were elevated
401 in disease, they were highly abundant in all the samples, and this correlation was not as dramatic
402 as that of *Rothia* and *Haemophilus* with health, indicating that the positive effects of *Rothia* and
403 *Haemophilus* may be more important than the negative effects of *Prevotella*. In a recent study,
404 *Rothia dentocariosa* and *Rothia aeria* were associated with good dental health (31), while in
405 another study *R. dentocariosa* was associated caries (56), indicating that the role of this genera

406 in caries development remains nebulous. The genera *Rothia*, *Neisseria*, and *Haemophilus* were
407 recently documented to be important mediators of cell-cell interactions within the early biofilm
408 derived from healthy individuals (57), are among the first colonizers of the oral cavity after birth
409 (58), and they were indeed largely health-associated in this study. As with *Rothia*, *Prevotella* spp.
410 have been associated with both health and dental caries, depending on the study. Our findings
411 are in line with several studies that associated *Prevotella* with dental caries (21, 59-61), including
412 one that found it was the best predictor of childhood caries (59). These reports were in contrast
413 to a study where *Prevotella* were enriched in the healthy cohort (62). The significant elevation in
414 the ratio of *Prevotella* to *Rothia* observed here may represent a useful novel biomarker for caries,
415 but wider studies are needed because the present study group was rather homogenous in terms
416 of host ethnicity and geography.

417 Although the alpha diversity of the caries group was not significantly lower when species-
418 level taxonomy was examined, alpha diversity was significantly reduced in the caries group when
419 functional pathways were examined. Overall, the functional analyses indicated that the presence
420 of several pathways is enriched in health, while there were no pathways detected by these
421 methods that were unequivocally enriched in disease. Contributional diversity (i.e. how many
422 taxa contribute a particular pathway to the community)(34) was reduced in the caries group. This
423 was particularly evident in the aerobic respiration performed by the health-associated *Neisseria*,
424 and several pathways that have been previously associated with the forestalling of caries
425 pathogenesis including arginine (35) and BCAA pathways (37), which both release alkaline
426 molecules that serve to buffer the environment and prevent enamel demineralization (63).

427 A number of previous studies have illustrated that penetration of the dental plaque
428 infection into the dentin is associated with elevation of a number of cytokines and host signaling
429 molecules (64-70). Several of these reports were supported here, where 10 immunological
430 factors were observed at significantly elevated concentrations in the caries group compared to
431 the healthy group. These molecules have an array of functions, and are likely to themselves

432 influence the microbiota of the oral cavity (71). Microbe-host immunological marker co-
433 occurrences have been characterized in periodontitis (72-74), but have not been previously
434 examined in dental caries. Machine learning was employed to examine these microbe-molecule
435 co-occurrences for the first time. Interestingly, the caries associated *Prevotella histicola*,
436 *Prevotella salivae*, and *Veillonella atypica* co-occurred frequently with EGF, IL-1RA, and TGF α ,
437 which were all themselves caries associated. While this co-occurrence data provides an obvious
438 chicken or egg dilemma (and it is likely that this cross-talk is bi-directional), it also provides an
439 atlas of microbe-host metabolite interactions that are most likely to be critical to the dysbiosis
440 involved in caries pathogenesis, and which deserve more in-depth analysis. EGF was one of the
441 markers most significantly elevated in the caries group, and has been previously documented to
442 be incorporated into dentin and released on orthodontic force (75).

443 A further advantage of metagenomic sequencing is the ability to assemble MAGs, which
444 allow further analysis of pan-genomics, and the identification of novel taxa. Excitingly, of the 527
445 MAGs reported in this study, 20% (98 MAGs) represented novel taxa, including 23 putative novel
446 genera. 8 FGBs, representing new genera, were CPR bacteria, including Saccharibacteria and
447 Gracilibacteria. Novel genera and species were also identified within more well-characterized
448 genera including Prevotellaceae, Porphyromonadaceae. Several of these novel genomes,
449 including uSGBs of *Peptostreptococcus*, *Solobacterium*, and *Lachnospiraceae* were assembled
450 and binned from a large number of subjects independently, indicating that these unknown taxa
451 may be widespread in the study population. The wealth of detailed genomic information provided
452 by this study invites deeper analysis into the pan-genomes of the various SGBs, and investigation
453 into the relationship of certain genotypes with disease status.

454 The execution of the genomics portion of this study highlighted several issues facing
455 microbial genomics studies. One predicament is the large and growing number of databases
456 containing genome sequences from which to choose from, as well as the quality of the contents
457 of these repositories and maintenance of up-to-date naming and taxonomic information. An

458 example was that the *Alloprevotella tanneriae* genomes in this study initially annotated as
459 *Prevotella tanneriae* due to the naming used by the RefSeq database, despite the recognition of
460 *Alloprevotella* as a distinct genus for several years (76). This is a particularly difficult issue to
461 address, as changes to established phylogeny are frequent and occasionally controversial; in fact
462 a recent study proposed a large overhaul of the bacterial tree of life, with 58% of taxa being
463 reclassified (77). Timely implementation of improved phylogeny will help solve another issue
464 noted in this study, the polyphyly of many taxonomic groups, particularly the class Clostridiales.
465 Further, as mentioned above, the use of 95% ANI as the cutoff to define a species remains
466 somewhat controversial, despite increased use and supporting evidence (42). There were
467 several rare occasions in this dataset where SGBs, as defined by the 95% ANI distance matrix,
468 included MAGs that best matched different (although closely related) RefSeq references.
469 Whether this indicates that 95% ANI is not stringent enough (e.g. these should in fact be classified
470 as multiple species) or too stringent (e.g. they should all be classified as the same species) is a
471 debate beyond the scope of this work. It is also likely that different taxa have disparate
472 pangenomic plasticities. Additionally, similar cutoffs and definitions for genus, family, etc. are
473 even less well-established (77), leaving a large amount of room for interpretation with large scale
474 studies where high numbers of novel taxa are described.

475 Overall, this study provided a plethora of data regarding the oral microbiome during dental
476 caries, and its co-occurrences with host immunological markers. The tools utilized to analyze
477 correlation to between taxa or functional pathways and disease status, as well as host markers,
478 were designed specifically to be robust for the compositional data provided by sequencing. The
479 authors envision the bioinformatics pipelines employed here are a useful template to guide further
480 studies of the oral microbiome. Application of these analyses to larger and more diverse samples
481 will dramatically improve our understanding of oral microbial ecology, and influence of the human
482 host during dental caries.

483

484 **MATERIALS AND METHODS**

485

486 **Ethics statement.** Child participants and parents understood the nature of the study, and
487 parents/guardians provided informed consent prior to the commencement of the study. The Ethics
488 Committees of the School of Dentistry, University of California, Los Angeles, CA, USA and the J.
489 Craig Venter Institute, La Jolla, CA, USA, approved the study design as well as the procedure for
490 obtaining informed consent (IRB reference numbers: 13-001075 and 2016-226). All experiments
491 were performed in accordance with the approved guidelines.

492

493 **Study Design.** Subjects were included in the study if the subject was 3 years old or older, in
494 good general health according to a medical history and clinical judgment of the clinical
495 investigator, and had at least 12 teeth. Subjects were excluded from the study if they had
496 generalized rampant dental caries, chronic systemic disease, or medical conditions that would
497 influence the ability to participate in the proposed study (i.e., cancer treatment, HIV, rheumatic
498 conditions, history of oral candidiasis). Subjects were also excluded if they had open sores or
499 ulceration in the mouth, radiation therapy to the head and neck region of the body, significantly
500 reduced saliva production or had been treated by anti-inflammatory or antibiotic therapy in the
501 past 6 months. Ethnic origin was mixed for healthy subjects (Hispanic, Asian, Caucasian,
502 Caucasian/Asian), while children with caries were of Hispanic origin. For the latter group, no other
503 ethnic group enrolled despite several attempts to identify interested families/participants. Children
504 with both primary and mixed dentition stages were included (caries group: 18 children with mixed
505 dentition and 6 with primary dentition; healthy group: 19 children with mixed dentition and 6 with
506 primary dentition). To further enable classification of health status (here caries and healthy), a
507 comprehensive oral examination of each subject was performed as described below. Subjects
508 were dichotomized into two groups: caries free (dmft/DMFT = 0) and caries active (subjects with
509 ≥ 2 active dentin lesions). If the subject qualified for the study, (s)he was to abstain from oral

510 hygiene activity, and eating and drinking for 2 hours prior to saliva collection in the morning. An
511 overview of the subjects and associated metadata is provided in Table S1.

512 i. *Comprehensive oral examination and study groups.* The exam was performed by a single
513 calibrated pediatric dental resident (RA), using a standard dental mirror, illuminated by artificial
514 light. The visual inspection was aided by tactile inspection with a community periodontal index
515 (CPI) probe when necessary. Radiographs (bitewings) were taken to determine the depth of
516 carious lesions. The number of teeth present was recorded and their dental caries status was
517 recorded using decayed (d), missing due to decay (m), or filled (f) teeth in primary and permanent
518 dentitions (dmft/DMFT), according to the criteria proposed by the World Health Organization
519 (1997) (78). Duplicate examinations were performed on 5 randomly selected subjects to assess
520 intra-examiner reliability. Subjects were dichotomized into two groups: caries free (CF;
521 dmft/DMFT=0) and caries active (CA; subjects with ≥ 2 active dentin lesions). The gingival health
522 condition of each subject was assessed using the Gingival Index (GI) (79). GI data was published
523 previously (80). Additionally, parent/guardian of each participant completed a survey regarding
524 oral health regimen.

525 ii. *Radiographic Assessment.* Bitewing radiographs were analyzed on the XDR Imaging Software
526 (Los Angeles, CA). Lesion depth was determined with the measuring tool, and categorized as
527 follows: E1 (radiolucency extends to outer half of enamel), E2 (radiolucency may extend to the
528 dentinoenamel junction), D1 (radiolucency extends to the outer one-third of dentin), D2
529 (radiolucency extends into the middle one third of dentin), and D3 (radiolucency extends into the
530 inner one third of dentin)(81). To calculate the depth of lesion score, the following scores were
531 assigned to each lesion depth: E1 = 1, E2 = 2, D1 = 3, D2 = 4, and D3 = 5, afterwards a total
532 depth score was calculated for each subject.

533 iii. *Saliva Collection.* Unstimulated saliva was collected between 8:00-11:00am for the salivary
534 immunological markers analysis. Subjects were asked to abstain from oral hygiene activity, and
535 eating and drinking for two hours prior to collection. Before collection, subjects were instructed to

536 rinse with water to remove all saliva from the mouth. In this study, unstimulated saliva was
537 collected for salivary immunological marker analysis, while stimulated saliva (by chewing on
538 sterile parafilm) was collected for Illumina sequencing (to dilute and amount of human DNA and
539 material present). 2 ml of unstimulated saliva was collected from subjects by drooling/spitting
540 directly into a 50mL Falcon conical tube (Fisher Scientific, Pittsburg PA) at regular intervals for a
541 period of 5-20 minutes. Saliva samples were immediately placed on ice and protease inhibitor
542 cocktail (Sigma, MO, USA) was added at a ratio of 100uL per 1mL of saliva to avoid protein
543 degradation. Then saliva samples were processed by centrifugation at 6,000 x g for 5 min at 4°C,
544 and the supernatants were transferred to cryotubes. The samples were immediately frozen in
545 liquid nitrogen and stored at -80 °C until analysis. 2 ml of stimulated saliva was collected
546 immediately following collection of unstimulated saliva.

547

548 **Salivary Immunological Biomarker Analysis.** Frozen unstimulated saliva samples were
549 thawed and processed through high-speed ultracentrifugation to precipitate cells and mucin for
550 extraction of proteins. Host immunological marker profiles were determined by Multiplexed
551 Luminex bead immunoassay (Westcoast Biosciences, San Diego, CA). A total of 38 analytes
552 were measured, the specific immune biomarkers that were studied in saliva samples included:
553 Epidermal Growth Factor (EGF), Fibroblast Growth Factor-2 (FGF-2), Eotaxin, Transforming
554 Growth Factor alpha (TGF- α), Granulocyte Colony-Stimulating Factor (G-CSF), Granulocyte-
555 Macrophage Colony-Stimulating Factor (GM-CSF), FMS-Like Tyrosine Kinase 3 Ligand (Flt-3L),
556 Vascular Endothelial Growth Factor (VEGF), Fractalkine, Growth-Regulated Oncogene (GRO),
557 Monocyte-Chemotactic Protein 3 (MCP-3), Macrophage-Derived Chemokine (MDC), Interleukin-
558 8 (IL-8), Protein 10 (IP-10), Monocyte Chemotactic Protein-1 (MCP-1), Macrophage Inflammatory
559 Protein-1 alpha (MIP-1 α), Macrophage Inflammatory Protein-1 beta (MIP-1 β), Interferon Alpha2
560 (IFN- α 2), Interferon gamma (IFN- γ), Interleukin-1 alpha (IL-1 α), Interleukin-1 beta (IL-1 β),

561 Interleukin-1 Receptor Antagonist (IL-1RA), Interleukin-2 (IL-2), Interleukin-3 (IL-3), Interleukin-4
562 (IL-4), Interleukin-5 (IL-5), Interleukin-6 (IL-6), Interleukin-7 (IL-7), Interleukin-9 (IL-9), Interleukin-
563 10 (IL-10), Interleukin-12(p40) (IL-12(p40)), Interleukin-12(p70) (IL-12(p70)), Interleukin-13 (IL-
564 13), Interleukin-15 (IL-15), Interleukin-17 (IL-17), Soluble CD40 Ligand (sCD40L), Tumor
565 Necrosis Factor-alpha (TNF- α), Tumor Necrosis Factor-beta (TNF- β). Quantities of each host
566 marker were compared between healthy and caries groups. In the cases of eotaxin, sCD40L, IL-
567 17A, IL-9, IL-2, IL-3, and IL-4, the majority of samples contained levels of the respective molecule
568 below the limit of detection for the assay. Therefore, these salivary immunological markers were
569 not analyzed subsequently. After removal of outliers using the ROUT method with a Q = 1%, a
570 Welch's t-test was used to determine significantly differentially abundant immunological markers.
571

572 **DNA Extraction and sequencing.** Frozen stimulated saliva samples were thawed on ice. DNA
573 was extracted and purified from the supernatant by employing QIAmp microbiome (Qiagen) and
574 DNA clean & concentrator (Zymo Research) kit procedures where host nucleic acid depletion step
575 was skipped to maximize bacterial DNA recovery. Libraries were prepared using Illumina
576 NexteraXT DNA library preparation kit according to the manufacturer's instructions. Sequencing
577 was carried out at the J. Craig Venter Institute (JCVI) Joint Technology Center (JTC) by using an
578 Illumina NextSeq 500 platform (San Diego, CA, USA) (150 bp paired end reads). DNA sample
579 concentrations were normalized at prior to sequencing. For 45 of the 47 samples, sequencing
580 depth was 5-31 million reads per sample. Two samples, SC40 (caries) and SC33 (healthy) were
581 sequenced ultra-deep, to 366 and 390 million reads, respectively, to examine the what information
582 can be gleaned from even deeper sequencing. The number of reads is listed in Table S12.

583

584 **Bioinformatics analysis.**

585 i. *Quality Control.* Raw Illumina reads were subjected to quality filtering and barcode trimming
586 using KneadData v0.5.4 (available at <https://bitbucket.org/biobakery/kneaddata>) by employing

587 trimmomatic settings of 4-base wide sliding window, with average quality per base >20 and
588 minimum length 90 bp. Reads mapping to the human genome were also removed. KneadData
589 quality control information is provided in Table S12.

590

591 ii. *Taxonomy of reads.* Filtered reads were then analyzed using MetaPhlan2 v2.7.5 (28) to
592 determine relative abundances of taxa. A custom script was used to obtain an estimated number
593 of reads using the relative abundances of each taxa and the predicted total number of reads from
594 each sample based on MetaPhlan2.

595

596 iii. *Calculation of beta diversity with feature loadings.* The taxonomic abundance table (i.e. OTU
597 table) generated from MetaPhlan2 was used as input for the QIIME2 (29) plugin, DEICODE (30),
598 which used Robust Aitchison PCA to calculate beta diversity with feature loadings. The resulting
599 biplot was visualized using the QIIME2 plugin Emperor (39). The feature loadings for Axis 2 of
600 the biplot (the axis with the most difference in disease status) were visualized using Qurro
601 (doi:10.5281/zenodo.3369454).

602

603 iv. *Using reference frames to identify taxa associated with disease.* The OTU table generated by
604 MetaPhlan2 was used as input for Songbird (13) in order to rank species association with disease
605 status. The following parameters were used: number of random test examples: 5, epochs:
606 50,000, batch size: 3, differential-prior: 1, learning rate: 0.001. The resulting differentials were
607 visualized using Qurro.

608

609 v. *Functional profiling of metagenomes.* HUMAnN2 (34) was used to provide information about
610 the functional pathways present in the metagenomes. DEICODE was utilized analyze the
611 relationship between particular metabolic pathways and disease status and Emperor was used to
612 visualize the resulting ordination. Songbird was utilized to rank the pathways in terms of

613 association with disease status using the same parameters described above and the ranks were
614 visualized with Qurro.

615

616 vi. *Estimation of species-saliva immunological marker co-occurrence.* The co-occurrence of
617 species and immunological markers was estimated using neural networks via mmvec
618 (<https://github.com/biocore/mmvec>). The following parameters were used: number of testing
619 examples: 5, minimum feature count: 10, epochs: 1000, batch size: 3, latent dim: 3, input prior: 1,
620 output prior: 1, learning rate 0.001. Emperor was used to visualize the resulting biplot.

621

622 vii. *Assembly and binning of MAGs.* metaSPAdes was utilized to *de novo* assemble
623 metagenomes from the quality-filtered Illumina reads (82). The resulting assemblies were binned
624 using the MetaWRAP pipeline v1.1.5 (83). The MetaWRAP initial_binning module used Maxbin2,
625 Metabat2, and Concoct. Subsequently, the bin_refinement module was used to construct the
626 best final bin set by comparing the results of the 3 binning tools. The bin_reassembly module
627 was then used to reassemble the final bin set to make further improvements. The quality control
628 cutoffs for all MetaWRAP modules were >50% completeness and <10% contamination, which are
629 the cutoffs for Medium-Quality Draft Metagenome-Assembled Genomes as set forth by the
630 Genome Standards Consortium (40). This generated 527 metagenome-assembled genomes
631 (MAGs) that were at least of medium quality. The classify_bins and quant_bins modules were
632 used to respectively obtain a taxonomy estimate based on megablast and to provide the quantity
633 of each bin in the form of 'genome copies per million reads'.

634

635 viii. *Determining species level genome bins.* To identify species-level genome bins (SGBs), Mash
636 v2.1 (43) was used to query all 527 MAGs against the entire RefSeq database with a Mash
637 distance cutoff of 5 (corresponding to a 95% average nucleotide identity (ANI)). Although a topic
638 of some debate, 95%ANI has been used by several recent landmark studies as the cutoff for

639 genomes representing the same species. All MAGs with a RefSeq hit with a Mash distance of <5
640 were assigned the species name of that hit. Because Mash can underestimate ANI for less than
641 complete genomes, fastANI v1.1 was used to compare the ANI of all 570 MAGs and generate a
642 distance matrix. This distance matrix was used to create a Cytoscape network to visualize all
643 MAGs that had an ANI>95% (i.e. link all bins that were of the same species, based on ANI, with
644 an edge). The fact that Mash distance <5 and fastANI ANI>95% aligned almost perfectly served
645 as a useful internal control. This strategy resulted in 151 SGB's (91 with no connection and 60
646 with at least one). 95 SGBs, representing 444 total bins (MAGs), had a Mash and/or fastANI hit
647 with ANI >95%, and were termed known SGBs (kSGBs). 56 of the total SGBs, representing 126
648 total bins (MAGs), did not have hit in RefSeq with at least 95%ANI and therefore were defined as
649 unknown SGBs (uSGBs). To further define the uSGBs, a combination of Mash distances < 30 to
650 the RefSeq database, CheckM, the metaWRAP classify_bins module (which uses taxator TK),
651 fastANI, Kraken, and blastx were used to determine the taxonomy of the uSGBs. When uSGBs
652 contained multiple MAGs, the MAG with the best quality score according to the formula
653 (completion – (2x contamination)) was used to find the best hit. Previous studies have utilized
654 ANI cutoffs of 85% and 70% to determine genus and family level genome bins, and a similar
655 approach was used here with manual evaluation of the closest ANI hits leading to assignment of
656 uSGBs to genus-level genome bins (GGBs) or family level genome bins (FGBs).

657
658 ix. *Phylogenetic placement of uSGBs.* PhyloPhlAn2 (41) was used to determine the phylogeny
659 of uSGBs. The following parameters were used: --diversity medium --accurate. The following
660 external tools were used: diamond (84), mafft (85), trimal (86), fasttree (87), and RAxML (88).
661 Resulting phylogenetic trees were visualized using iTOL 4.(89)

662
663 x. *Inference of actively replicating taxa.* iRep (49) was utilized to infer the replication rates of taxa
664 in the metagenomes assembled using metaSPAdes as described above. iRep was then used to

665 calculate the estimated replication rate of genera for which sufficient draft genomes had been
666 assembled from the metagenomic data.

667

668 **Data availability.** Sequence data have been submitted to NCBI under BioProject ID
669 PRJNA478018 with SRA accession number SRP151559. MAGs have been uploaded to PATRIC
670 and annotated (will be made public upon acceptance for publication).

671

672

673

674 **ACKNOWLEDGEMENTS**

675 This study was supported by NIH/NIDCR grants F32-DE026947 (J.L.B.) and R00-DE024543

676 (A.E.). The authors also acknowledge and thank R. Alexander Richter, Semar Petrus, Josh

677 Espinoza, Drishti Kaul, Clarisse Marotz, Marcus Fedarko, and Cameron Martino for very helpful

678 scientific discussions.

679

680 **FIGURE LEGENDS**

681

682 **Fig 1. Overview of study design and bioinformatics methods.** (A) Flow chart illustrating the
683 steps taken to get from clinical specimen to bioinformatics data. (B) Flow chart illustrating the
684 computational methodology utilized in this study. Input data is in yellow boxes, intermediate data
685 is in blue boxes, and final data is in green boxes. For each step, the tool(s) or package(s) used
686 are provided in italics. The 'Final bins with taxonomy' box is color-coded to match the
687 metagenome-assembled genome (MAG) average nucleotide (ANI) network in Figure 5.

688

689 **Fig 2. Significant taxonomic differences in the oral metagenome between healthy children**
690 **and children with caries.** (A) **Species abundance.** Phylogenetic tree illustrating the species
691 present across the saliva metagenomes. The relative abundance of each taxa is represented by
692 the bar graph at the end of each leaf, with the relative abundance in the healthy group in blue and
693 the caries group in red. Taxa of interest are highlighted with colored leaves on the tree:
694 *Streptococcus mutans* and *Streptococcus sobrinus* = yellow; *Prevotella* spp.= red; and *Rothia*
695 spp. = green. (B) **Beta Diversity.** Compositional biplot visualized in Emperor (39) and generated
696 using DEICODE (robust Aitchison PCA)(30). Data points represent individual subjects and are
697 colored with a gradient to visualize DMFT score, indicating severity of dental caries. Feature
698 loadings (i.e. taxa driving differences in ordination space) are illustrated by the vectors, which are
699 labeled with the cognate species name. (C) **Ranking of RPCA Axis 2 feature loadings.** Qurro-
700 produced bar chart illustrating the sorted ranks of the feature loadings of Axis 2 from Figure 1B,
701 corresponding to the main RPCA space separation between the healthy and caries groups.
702 *Prevotella* spp. are highlighted in red, while *Rothia* spp. are highlighted in green, *S. mutans* is
703 highlighted in yellow, *Haemophilus* spp. are highlighted in dark blue, and *Neisseria* spp. are
704 highlighted in light blue. (D) **Differential rankings of taxa associated with disease status.**
705 Qurro-produced bar chart illustrating the sorted differential rankings of taxa associated with

706 disease status determined by Songbird (13). *Prevotella* spp. are highlighted in red, *Rothia* spp.
707 are highlighted in green, and *S. mutans* is highlighted in yellow, *Haemophilus* spp. are highlighted
708 in dark blue, and *Neisseria* spp. are highlighted in light blue. **(E) The log-ratio of *Prevotella***
709 **spp./*Rothia* spp. is significantly increased in caries.** Bar chart illustrating the log₂ ratio of
710 *Prevotella* spp./*Rothia* spp. across the healthy and caries sample groups. **, denotes statistical
711 significance, based on a Welch's *t*-test ($p = 0.001$). No samples were dropped as all samples
712 contained these 4 taxa.

713
714 **Fig 3. Profiling of functional pathways illustrates differences between health- and caries-**
715 **associated oral microbiota. (A) A greater diversity of functional pathways are present in**
716 **the healthy group.** Bar chart illustrating the alpha diversity (Shannon Index) of the functional
717 pathways present in the healthy and caries groups, as determined by HUMAnN2 (34) analysis.
718 *, indicates statistical significance, based upon a Kruskal-Wallis test ($p = 0.0136$). **(B) Beta**
719 **diversity of functional pathways.** 3D PCA plot generated using DEICODE (robust Aitchison
720 PCA)(30). Data points represent individual subjects and are colored with a gradient to visualize
721 DMFT score, indicating severity of dental caries. Feature loadings (i.e. functional pathways
722 driving differences in ordination space) are illustrated by the vectors, which are labeled with the
723 cognate pathway name. **(C) Contributinal diversity of 69 core pathways.** Scatter plot
724 indicating alpha and beta diversities of 69 functional pathways which were found across all
725 samples. **(D-H) Contributinal diversity of pathways of interest to caries pathogenesis.**
726 Stacked bar charts illustrating the relative abundance and contributinal diversity of the indicated
727 pathways across the samples (D, L-arginine biosynthesis I; E, L-arginine biosynthesis II; F,
728 branched chain amino acid biosynthesis).

729
730 **Fig 4. Significant differences in the salivary immunological profile of healthy children and**
731 **children with caries. (A-J) Swarm plots illustrating the 10 immunological markers, (A) EGF, (B)**

732 IL-10, **(C)** G-CSF, and **(D)** IL1-RA, **(E)** IL-15, **(F)** TGF α , **(G)** GM-CSF, **(H)** MDC, **(I)** IL-13, and **(J)**
733 IL-6, which were significantly different between healthy and caries subject groups. *, $p < 0.05$,
734 based on a Welch's t-test. **(K) Microbe-immune marker co-occurrence.** Biplot illustrating the
735 co-occurrence of oral taxa with immune markers. The 31 detected immune markers are
736 represented by spheres, while 15 bacterial taxa with high differential ranks are represented by
737 vectors. Red spheres indicate host markers that were elevated in caries, while blue spheres
738 indicate host markers that were not significantly different between caries and health. Vectors are
739 colored by Songbird ranks (Figure 2D) indicating association with caries versus health. Several
740 immunological markers of interest are labeled.

741
742 **Fig 5. 527 metagenome-assembled genomes (MAGs) were recovered. (A) Recovery of**
743 **151 species-level genome bins (SGBs), representing 527 MAGs and ~50 novel taxa.**
744 Network representing an average nucleotide identity (ANI) distance matrix, generated by fastANI
745 (42). Nodes represent MAGs, while edges represent an ANI > 95% (the cutoff chosen to
746 designate species boundaries in this study). Circular nodes indicate MAGs recovered from
747 healthy samples, while chevrons indicate MAGs recovered from caries samples. Nodes are
748 colored based upon bin designation: species-level (SGB: known species; yellow), genus-level
749 (GGB: known genus, novel species; blue), family-level (FGB: novel genus and species, green),
750 or reassigned to SGB (described in Fig. 1; orange, Table S). Sub-networks of interest are labeled
751 with taxonomic names. **(B-E) Statistics indicating MAG quality.** Violin charts illustrating the
752 Completion **(B)**, N50 **(C)**, Contamination **(D)**, and contigs/Mbp **(E)** of the SGBs, GGBs, and FGBs.
753 (completion and contamination were determined by CheckM (90)). Asterisks indicate statistical
754 significance between indicated groups, based upon a Tukey's Multiple Comparisons Test
755 following a one-way ANOVA. *, $p < 0.05$; **, $p < 0.01$; ****, $p < 0.0001$ **(F-H) Phylogenetic trees**
756 **of Saccharibacteria (F), Bacteroidales (G), and Clostridiales (H) reference genomes with**

757 **placement of uSGBs.** GGBs, FGBs, and SGBs (Saccharibacteria only) are denoted by stars of

758 the indicated color. Trees were constructed using PhyloPhAn2.

759

760 REFERENCES

761

- 762 1. Pitts NB, Zero DT, Marsh PD, Ekstrand K, Weintraub JA, Ramos-Gomez F, Tagami J,
763 Twetman S, Tsakos G, Ismail A. 2017. Dental caries. *Nat Rev Dis Primers* 3:17030.
- 764 2. Loesche WJ. 1986. Role of *Streptococcus mutans* in human dental decay. *Microbiol Rev*
765 50:353-80.
- 766 3. Simon-Soro A, Mira A. 2015. Solving the etiology of dental caries. *Trends Microbiol*
767 23:76-82.
- 768 4. Bowen WH, Burne RA, Wu H, Koo H. 2018. Oral Biofilms: Pathogens, Matrix, and
769 Polymicrobial Interactions in Microenvironments. *Trends Microbiol* 26:229-242.
- 770 5. Burne RA. 2018. Getting to Know "The Known Unknowns": Heterogeneity in the Oral
771 Microbiome. *Adv Dent Res* 29:66-70.
- 772 6. Cross B, Faustoferri RC, Quivey RG, Jr. 2016. What are We Learning and What Can We
773 Learn from the Human Oral Microbiome Project? *Curr Oral Health Rep* 3:56-63.
- 774 7. Mira A. 2018. Oral Microbiome Studies: Potential Diagnostic and Therapeutic
775 Implications. *Adv Dent Res* 29:71-77.
- 776 8. Philip N, Suneja B, Walsh L. 2018. Beyond *Streptococcus mutans*: clinical implications of
777 the evolving dental caries aetiological paradigms and its associated microbiome. *Br Dent*
778 *J* 224:219-225.
- 779 9. Banas JA, Drake DR. 2018. Are the mutans streptococci still considered relevant to
780 understanding the microbial etiology of dental caries? *BMC Oral Health* 18:129.
- 781 10. Gloor GB, Macklaim JM, Pawlowsky-Glahn V, Egozcue JJ. 2017. Microbiome Datasets Are
782 Compositional: And This Is Not Optional. *Front Microbiol* 8:2224.
- 783 11. Morton JT, Sanders J, Quinn RA, McDonald D, Gonzalez A, Vazquez-Baeza Y, Navas-
784 Molina JA, Song SJ, Metcalf JL, Hyde ER, Lladser M, Dorrestein PC, Knight R. 2017.
785 Balance Trees Reveal Microbial Niche Differentiation. *mSystems* 2.
- 786 12. Knight R, Vrbanac A, Taylor BC, Aksenov A, Callewaert C, Debelius J, Gonzalez A,
787 Kosciolk T, McCall LI, McDonald D, Melnik AV, Morton JT, Navas J, Quinn RA, Sanders
788 JG, Swafford AD, Thompson LR, Tripathi A, Xu ZZ, Zaneveld JR, Zhu Q, Caporaso JG,
789 Dorrestein PC. 2018. Best practices for analysing microbiomes. *Nat Rev Microbiol*
790 16:410-422.
- 791 13. Morton JT, Marotz C, Washburne A, Silverman J, Zaramela LS, Edlund A, Zengler K,
792 Knight R. 2019. Establishing microbial composition measurement standards with
793 reference frames. *Nat Commun* 10:2719.
- 794 14. Hong S, Bunge J, Leslin C, Jeon S, Epstein SS. 2009. Polymerase chain reaction primers
795 miss half of rRNA microbial diversity. *ISME J* 3:1365-73.
- 796 15. Pinto AJ, Raskin L. 2012. PCR biases distort bacterial and archaeal community structure
797 in pyrosequencing datasets. *PLoS One* 7:e43093.
- 798 16. Jovel J, Patterson J, Wang W, Hotte N, O'Keefe S, Mitchel T, Perry T, Kao D, Mason AL,
799 Madsen KL, Wong GK. 2016. Characterization of the Gut Microbiome Using 16S or
800 Shotgun Metagenomics. *Front Microbiol* 7:459.
- 801 17. Louca S, Doebeli M, Parfrey LW. 2018. Correcting for 16S rRNA gene copy numbers in
802 microbiome surveys remains an unsolved problem. *Microbiome* 6:41.

- 803 18. Human Microbiome Project C. 2012. Structure, function and diversity of the healthy
804 human microbiome. *Nature* 486:207-14.
- 805 19. Langille MG, Zaneveld J, Caporaso JG, McDonald D, Knights D, Reyes JA, Clemente JC,
806 Burkepille DE, Vega Thurber RL, Knight R, Beiko RG, Huttenhower C. 2013. Predictive
807 functional profiling of microbial communities using 16S rRNA marker gene sequences.
808 *Nat Biotechnol* 31:814-21.
- 809 20. Espinoza JL, Harkins DM, Torralba M, Gomez A, Highlander SK, Jones MB, Leong P,
810 Saffery R, Bockmann M, Kuelbs C, Inman JM, Hughes T, Craig JM, Nelson KE, Dupont CL.
811 2018. Supragingival Plaque Microbiome Ecology and Functional Potential in the Context
812 of Health and Disease. *MBio* 9.
- 813 21. Al-Hebshi NN, Baraniya D, Chen T, Hill J, Puri S, Tellez M, Hasan NA, Colwell RR, Ismail A.
814 2019. Metagenome sequencing-based strain-level and functional characterization of
815 supragingival microbiome associated with dental caries in children. *J Oral Microbiol*
816 11:1557986.
- 817 22. Belda-Ferre P, Alcaraz LD, Cabrera-Rubio R, Romero H, Simon-Soro A, Pignatelli M, Mira
818 A. 2012. The oral metagenome in health and disease. *ISME J* 6:46-56.
- 819 23. Belstrom D, Constancias F, Liu Y, Yang L, Drautz-Moses DI, Schuster SC, Kohli GS,
820 Jakobsen TH, Holmstrup P, Givskov M. 2017. Metagenomic and metatranscriptomic
821 analysis of saliva reveals disease-associated microbiota in patients with periodontitis
822 and dental caries. *NPJ Biofilms Microbiomes* 3:23.
- 823 24. Costalonga M, Herzberg MC. 2014. The oral microbiome and the immunobiology of
824 periodontal disease and caries. *Immunol Lett* 162:22-38.
- 825 25. Meyle J, Dommisch H, Groeger S, Giacaman RA, Costalonga M, Herzberg M. 2017. The
826 innate host response in caries and periodontitis. *J Clin Periodontol* 44:1215-1225.
- 827 26. Bowen WH. 2016. Dental caries - not just holes in teeth! A perspective. *Mol Oral*
828 *Microbiol* 31:228-33.
- 829 27. Baker JL, Edlund A. 2018. Exploiting the Oral Microbiome to Prevent Tooth Decay: Has
830 Evolution Already Provided the Best Tools? *Front Microbiol* 9:3323.
- 831 28. Truong DT, Franzosa EA, Tickle TL, Scholz M, Weingart G, Pasolli E, Tett A, Huttenhower
832 C, Segata N. 2015. MetaPhlan2 for enhanced metagenomic taxonomic profiling. *Nat*
833 *Methods* 12:902-3.
- 834 29. Bolyen E, Rideout JR, Dillon MR, Bokulich NA, Abnet CC, Al-Ghalith GA, Alexander H, Alm
835 EJ, Arumugam M, Asnicar F, Bai Y, Bisanz JE, Bittinger K, Brejnrod A, Brislawn CJ, Brown
836 CT, Callahan BJ, Caraballo-Rodriguez AM, Chase J, Cope EK, Da Silva R, Diener C,
837 Dorrestein PC, Douglas GM, Durall DM, Duvallet C, Edwardson CF, Ernst M, Estaki M,
838 Fouquier J, Gauglitz JM, Gibbons SM, Gibson DL, Gonzalez A, Gorlick K, Guo J, Hillmann
839 B, Holmes S, Holste H, Huttenhower C, Huttley GA, Janssen S, Jarmusch AK, Jiang L,
840 Kaehler BD, Kang KB, Keefe CR, Keim P, Kelley ST, Knights D, et al. 2019. Reproducible,
841 interactive, scalable and extensible microbiome data science using QIIME 2. *Nat*
842 *Biotechnol* 37:852-857.
- 843 30. Martino C, Morton JT, Marotz CA, Thompson LR, Tripathi A, Knight R, Zengler K. 2019. A
844 Novel Sparse Compositional Technique Reveals Microbial Perturbations. *mSystems* 4.

- 845 31. Agnello M, Marques J, Cen L, Mittermuller B, Huang A, Chaichanasakul Tran N, Shi W, He
846 X, Schroth RJ. 2017. Microbiome Associated with Severe Caries in Canadian First Nations
847 Children. *J Dent Res* 96:1378-1385.
- 848 32. Thomas RZ, Zijngje V, Cicek A, de Soet JJ, Harmsen HJ, Huysmans MC. 2012. Shifts in the
849 microbial population in relation to in situ caries progression. *Caries Res* 46:427-31.
- 850 33. Pereira D, Seneviratne CJ, Koga-Ito CY, Samaranayake LP. 2018. Is the oral fungal
851 pathogen *Candida albicans* a cariogen? *Oral Dis* 24:518-526.
- 852 34. Franzosa EA, McIver LJ, Rahnnavard G, Thompson LR, Schirmer M, Weingart G, Lipson KS,
853 Knight R, Caporaso JG, Segata N, Huttenhower C. 2018. Species-level functional profiling
854 of metagenomes and metatranscriptomes. *Nat Methods* 15:962-968.
- 855 35. Nascimento MM, Alvarez AJ, Huang X, Hanway S, Perry S, Luce A, Richards VP, Burne RA.
856 2019. Arginine Metabolism in Supragingival Oral Biofilms as a Potential Predictor of
857 Caries Risk. *JDR Clin Trans Res* 4:262-270.
- 858 36. Fozo EM, Scott-Anne K, Koo H, Quivey RG, Jr. 2007. Role of unsaturated fatty acid
859 biosynthesis in virulence of *Streptococcus mutans*. *Infect Immun* 75:1537-9.
- 860 37. Santiago B, MacGilvray M, Faustoferri RC, Quivey RG, Jr. 2012. The branched-chain
861 amino acid aminotransferase encoded by *ilvE* is involved in acid tolerance in
862 *Streptococcus mutans*. *J Bacteriol* 194:2010-9.
- 863 38. Liu YL, Nascimento M, Burne RA. 2012. Progress toward understanding the contribution
864 of alkali generation in dental biofilms to inhibition of dental caries. *Int J Oral Sci* 4:135-
865 40.
- 866 39. Vazquez-Baeza Y, Pirrung M, Gonzalez A, Knight R. 2013. EMPeror: a tool for visualizing
867 high-throughput microbial community data. *Gigascience* 2:16.
- 868 40. Bowers RM, Kyrpides NC, Stepanauskas R, Harmon-Smith M, Doud D, Reddy TBK, Schulz
869 F, Jarett J, Rivers AR, Eloie-Fadrosch EA, Tringe SG, Ivanova NN, Copeland A, Clum A,
870 Becraft ED, Malmstrom RR, Birren B, Podar M, Bork P, Weinstock GM, Garrity GM,
871 Dodsworth JA, Yooseph S, Sutton G, Glockner FO, Gilbert JA, Nelson WC, Hallam SJ,
872 Jungbluth SP, Ettema TJG, Tighe S, Konstantinidis KT, Liu WT, Baker BJ, Rattei T, Eisen JA,
873 Hedlund B, McMahon KD, Fierer N, Knight R, Finn R, Cochrane G, Karsch-Mizrachi I,
874 Tyson GW, Rinke C, Genome Standards C, Lapidus A, Meyer F, Yilmaz P, Parks DH, et al.
875 2017. Minimum information about a single amplified genome (MISAG) and a
876 metagenome-assembled genome (MIMAG) of bacteria and archaea. *Nat Biotechnol*
877 35:725-731.
- 878 41. Pasolli E, Asnicar F, Manara S, Zolfo M, Karcher N, Armanini F, Beghini F, Manghi P, Tett
879 A, Ghensi P, Collado MC, Rice BL, DuLong C, Morgan XC, Golden CD, Quince C,
880 Huttenhower C, Segata N. 2019. Extensive Unexplored Human Microbiome Diversity
881 Revealed by Over 150,000 Genomes from Metagenomes Spanning Age, Geography, and
882 Lifestyle. *Cell* 176:649-662 e20.
- 883 42. Jain C, Rodriguez RL, Phillippy AM, Konstantinidis KT, Aluru S. 2018. High throughput ANI
884 analysis of 90K prokaryotic genomes reveals clear species boundaries. *Nat Commun*
885 9:5114.
- 886 43. Ondov BD, Treangen TJ, Melsted P, Mallonee AB, Bergman NH, Koren S, Phillippy AM.
887 2016. Mash: fast genome and metagenome distance estimation using MinHash.
888 *Genome Biol* 17:132.

- 889 44. Hug LA, Baker BJ, Anantharaman K, Brown CT, Probst AJ, Castelle CJ, Butterfield CN,
890 HERNSDORF AW, Amano Y, Ise K, Suzuki Y, Dudek N, Relman DA, Finstad KM, Amundson R,
891 Thomas BC, Banfield JF. 2016. A new view of the tree of life. *Nat Microbiol* 1:16048.
- 892 45. He X, McLean JS, Edlund A, Yooseph S, Hall AP, Liu SY, Dorrestein PC, Esquenazi E,
893 Hunter RC, Cheng G, Nelson KE, Lux R, Shi W. 2015. Cultivation of a human-associated
894 TM7 phylotype reveals a reduced genome and epibiotic parasitic lifestyle. *Proc Natl*
895 *Acad Sci U S A* 112:244-9.
- 896 46. Baker JL, Bor B, Agnello M, Shi W, He X. 2017. Ecology of the Oral Microbiome: Beyond
897 Bacteria. *Trends Microbiol* 25:362-374.
- 898 47. McLean JS, Bor B, To TT, Liu Q, Kerns KA, Solden L, Wrighton K, He X, Shi W. 2018.
899 Evidence of independent acquisition and adaptation of ultra-small bacteria to human
900 hosts across the highly diverse yet reduced genomes of the phylum Saccharibacteria.
901 *bioRxiv* doi:10.1101/258137:258137.
- 902 48. Wattam AR, Davis JJ, Assaf R, Boisvert S, Brettin T, Bun C, Conrad N, Dietrich EM, Disz T,
903 Gabbard JL, Gerdes S, Henry CS, Kenyon RW, Machi D, Mao C, Nordberg EK, Olsen GJ,
904 Murphy-Olson DE, Olson R, Overbeek R, Parrello B, Pusch GD, Shukla M, Vonstein V,
905 Warren A, Xia F, Yoo H, Stevens RL. 2017. Improvements to PATRIC, the all-bacterial
906 Bioinformatics Database and Analysis Resource Center. *Nucleic Acids Res* 45:D535-D542.
- 907 49. Brown CT, Olm MR, Thomas BC, Banfield JF. 2016. Measurement of bacterial replication
908 rates in microbial communities. *Nat Biotechnol* 34:1256-1263.
- 909 50. Kilian M, Chapple IL, Hannig M, Marsh PD, Meuric V, Pedersen AM, Tonetti MS, Wade
910 WG, Zaura E. 2016. The oral microbiome - an update for oral healthcare professionals.
911 *Br Dent J* 221:657-666.
- 912 51. Hillmann B, Al-Ghalith GA, Shields-Cutler RR, Zhu Q, Gohl DM, Beckman KB, Knight R,
913 Knights D. 2018. Evaluating the Information Content of Shallow Shotgun Metagenomics.
914 *mSystems* 3.
- 915 52. Almeida A, Mitchell AL, Boland M, Forster SC, Gloor GB, Tarkowska A, Lawley TD, Finn
916 RD. 2019. A new genomic blueprint of the human gut microbiota. *Nature* 568:499-504.
- 917 53. Nayfach S, Shi ZJ, Seshadri R, Pollard KS, Kyrpides NC. 2019. New insights from
918 uncultivated genomes of the global human gut microbiome. *Nature* 568:505-510.
- 919 54. Simon-Soro A, Belda-Ferre P, Cabrera-Rubio R, Alcaraz LD, Mira A. 2013. A tissue-
920 dependent hypothesis of dental caries. *Caries Res* 47:591-600.
- 921 55. Lemos JA, Palmer SR, Zeng L, Wen ZT, Kajfasz JK, Freires IA, Abranches J, Brady LJ. 2019.
922 The Biology of *Streptococcus mutans*. *Microbiol Spectr* 7.
- 923 56. Jiang S, Gao X, Jin L, Lo EC. 2016. Salivary Microbiome Diversity in Caries-Free and
924 Caries-Affected Children. *Int J Mol Sci* 17.
- 925 57. Palmer RJ, Jr., Shah N, Valm A, Paster B, Dewhirst F, Inui T, Cisar JO. 2017. Interbacterial
926 Adhesion Networks within Early Oral Biofilms of Single Human Hosts. *Appl Environ*
927 *Microbiol* 83.
- 928 58. Sulyanto RM, Thompson ZA, Beall CJ, Leys EJ, Griffen AL. 2019. The Predominant Oral
929 Microbiota Is Acquired Early in an Organized Pattern. *Sci Rep* 9:10550.
- 930 59. Teng F, Yang F, Huang S, Bo C, Xu ZZ, Amir A, Knight R, Ling J, Xu J. 2015. Prediction of
931 Early Childhood Caries via Spatial-Temporal Variations of Oral Microbiota. *Cell Host*
932 *Microbe* 18:296-306.

- 933 60. Hurley E, Barrett MPJ, Kinirons M, Whelton H, Ryan CA, Stanton C, Harris HMB, O'Toole
934 PW. 2019. Comparison of the salivary and dentinal microbiome of children with severe-
935 early childhood caries to the salivary microbiome of caries-free children. *BMC Oral*
936 *Health* 19:13.
- 937 61. Tanner AC, Kent RL, Jr., Holgerson PL, Hughes CV, Loo CY, Kanasi E, Chalmers NI,
938 Johansson I. 2011. Microbiota of severe early childhood caries before and after therapy.
939 *J Dent Res* 90:1298-305.
- 940 62. Gomez A, Espinoza JL, Harkins DM, Leong P, Saffery R, Bockmann M, Torralba M, Kuelbs
941 C, Kodukula R, Inman J, Hughes T, Craig JM, Highlander SK, Jones MB, Dupont CL, Nelson
942 KE. 2017. Host Genetic Control of the Oral Microbiome in Health and Disease. *Cell Host*
943 *Microbe* 22:269-278 e3.
- 944 63. Baker JL, Faustoferri RC, Quivey RG, Jr. 2017. Acid-adaptive mechanisms of
945 *Streptococcus mutans*-the more we know, the more we don't. *Mol Oral Microbiol*
946 32:107-117.
- 947 64. Adachi T, Nakanishi T, Yumoto H, Hirao K, Takahashi K, Mukai K, Nakae H, Matsuo T.
948 2007. Caries-related bacteria and cytokines induce CXCL10 in dental pulp. *J Dent Res*
949 86:1217-22.
- 950 65. Artese L, Rubini C, Ferrero G, Fioroni M, Santinelli A, Piattelli A. 2002. Vascular
951 endothelial growth factor (VEGF) expression in healthy and inflamed human dental
952 pulps. *J Endod* 28:20-3.
- 953 66. Kokkas AB, Goulas A, Varsamidis K, Mirtsou V, Tziafas D. 2007. Irreversible but not
954 reversible pulpitis is associated with up-regulation of tumour necrosis factor-alpha gene
955 expression in human pulp. *Int Endod J* 40:198-203.
- 956 67. McLachlan JL, Sloan AJ, Smith AJ, Landini G, Cooper PR. 2004. S100 and cytokine
957 expression in caries. *Infect Immun* 72:4102-8.
- 958 68. Hahn CL, Best AM, Tew JG. 2000. Cytokine induction by *Streptococcus mutans* and
959 pulpal pathogenesis. *Infect Immun* 68:6785-9.
- 960 69. Sloan AJ, Perry H, Matthews JB, Smith AJ. 2000. Transforming growth factor-beta
961 isoform expression in mature human healthy and carious molar teeth. *Histochem J*
962 32:247-52.
- 963 70. Horst OV, Horst JA, Samudrala R, Dale BA. 2011. Caries induced cytokine network in the
964 odontoblast layer of human teeth. *BMC Immunol* 12:9.
- 965 71. Chang AM, Liu Q, Hajjar AM, Greer A, McLean JS, Darveau RP. 2019. Toll-like receptor 2
966 and toll-like receptor 4 responses regulate neutrophil infiltration into the junctional
967 epithelium and significantly contribute to the composition of the oral microbiota. *J*
968 *Periodontol* doi:10.1002/JPER.18-0719.
- 969 72. Zhou J, Yao Y, Jiao K, Zhang J, Zheng X, Wu F, Hu X, Li J, Yu Z, Zhang G, Jiang N, Li Z. 2017.
970 Relationship between Gingival Crevicular Fluid Microbiota and Cytokine Profile in
971 Periodontal Host Homeostasis. *Front Microbiol* 8:2144.
- 972 73. Arias-Bujanda N, Regueira-Iglesias A, Alonso-Sampedro M, Gonzalez-Peteiro MM, Mira
973 A, Balsa-Castro C, Tomas I. 2018. Cytokine Thresholds in Gingival Crevicular Fluid with
974 Potential Diagnosis of Chronic Periodontitis Differentiating by Smoking Status. *Sci Rep*
975 8:18003.

- 976 74. Lundmark A, Hu YOO, Huss M, Johannsen G, Andersson AF, Yucel-Lindberg T. 2019.
977 Identification of Salivary Microbiota and Its Association With Host Inflammatory
978 Mediators in Periodontitis. *Front Cell Infect Microbiol* 9:216.
- 979 75. Derringer K, Linden R. 2007. Epidermal growth factor released in human dental pulp
980 following orthodontic force. *Eur J Orthod* 29:67-71.
- 981 76. Downes J, Dewhirst FE, Tanner AC, Wade WG. 2013. Description of *Alloprevotella rava*
982 gen. nov., sp. nov., isolated from the human oral cavity, and reclassification of *Prevotella*
983 *tanneriae* Moore et al. 1994 as *Alloprevotella tanneriae* gen. nov., comb. nov. *Int J Syst*
984 *Evol Microbiol* 63:1214-8.
- 985 77. Parks DH, Chuvochina M, Waite DW, Rinke C, Skarshewski A, Chaumeil PA, Hugenholtz
986 P. 2018. A standardized bacterial taxonomy based on genome phylogeny substantially
987 revises the tree of life. *Nat Biotechnol* 36:996-1004.
- 988 78. Organization WH. 1971. Oral health surveys: basic methods. World Health Organization.
- 989 79. Loe H. 1967. The Gingival Index, the Plaque Index and the Retention Index Systems. *J*
990 *Periodontol* 38:Suppl:610-6.
- 991 80. Aleti G, Baker JL, Tang X, Alvarez R, Dinis M, Tran NC, Melnik AV, Zhong C, Ernst M,
992 Dorrestein PC, Edlund A. 2019. Identification of the Bacterial Biosynthetic Gene Clusters
993 of the Oral Microbiome Illuminates the Unexplored Social Language of Bacteria during
994 Health and Disease. *MBio* 10.
- 995 81. Anusavice KJ. 2005. Present and future approaches for the control of caries. *J Dent Educ*
996 69:538-54.
- 997 82. Nurk S, Meleshko D, Korobeynikov A, Pevzner PA. 2017. metaSPAdes: a new versatile
998 metagenomic assembler. *Genome Res* 27:824-834.
- 999 83. Uritskiy GV, DiRuggiero J, Taylor J. 2018. MetaWRAP-a flexible pipeline for genome-
1000 resolved metagenomic data analysis. *Microbiome* 6:158.
- 1001 84. Buchfink B, Xie C, Huson DH. 2015. Fast and sensitive protein alignment using
1002 DIAMOND. *Nat Methods* 12:59-60.
- 1003 85. Katoh K, Standley DM. 2013. MAFFT multiple sequence alignment software version 7:
1004 improvements in performance and usability. *Mol Biol Evol* 30:772-80.
- 1005 86. Capella-Gutierrez S, Silla-Martinez JM, Gabaldon T. 2009. trimAl: a tool for automated
1006 alignment trimming in large-scale phylogenetic analyses. *Bioinformatics* 25:1972-3.
- 1007 87. Price MN, Dehal PS, Arkin AP. 2009. FastTree: computing large minimum evolution trees
1008 with profiles instead of a distance matrix. *Mol Biol Evol* 26:1641-50.
- 1009 88. Stamatakis A. 2014. RAxML version 8: a tool for phylogenetic analysis and post-analysis
1010 of large phylogenies. *Bioinformatics* 30:1312-3.
- 1011 89. Letunic I, Bork P. 2019. Interactive Tree Of Life (iTOL) v4: recent updates and new
1012 developments. *Nucleic Acids Res* 47:W256-W259.
- 1013 90. Parks DH, Imelfort M, Skennerton CT, Hugenholtz P, Tyson GW. 2015. CheckM: assessing
1014 the quality of microbial genomes recovered from isolates, single cells, and
1015 metagenomes. *Genome Res* 25:1043-55.
- 1016

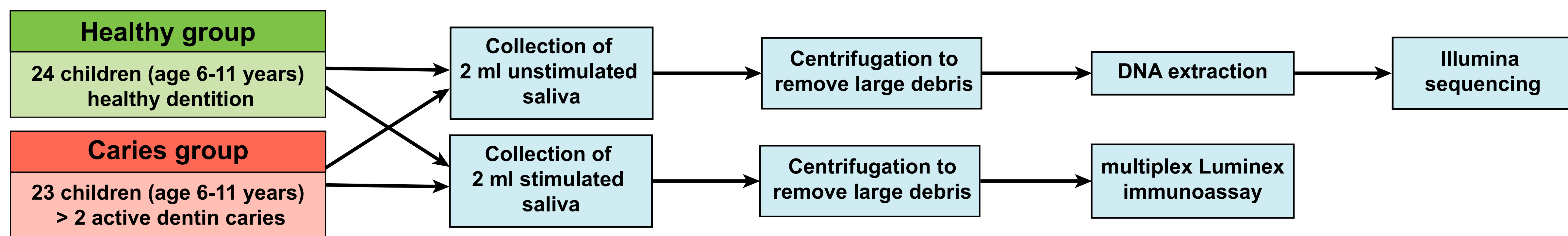
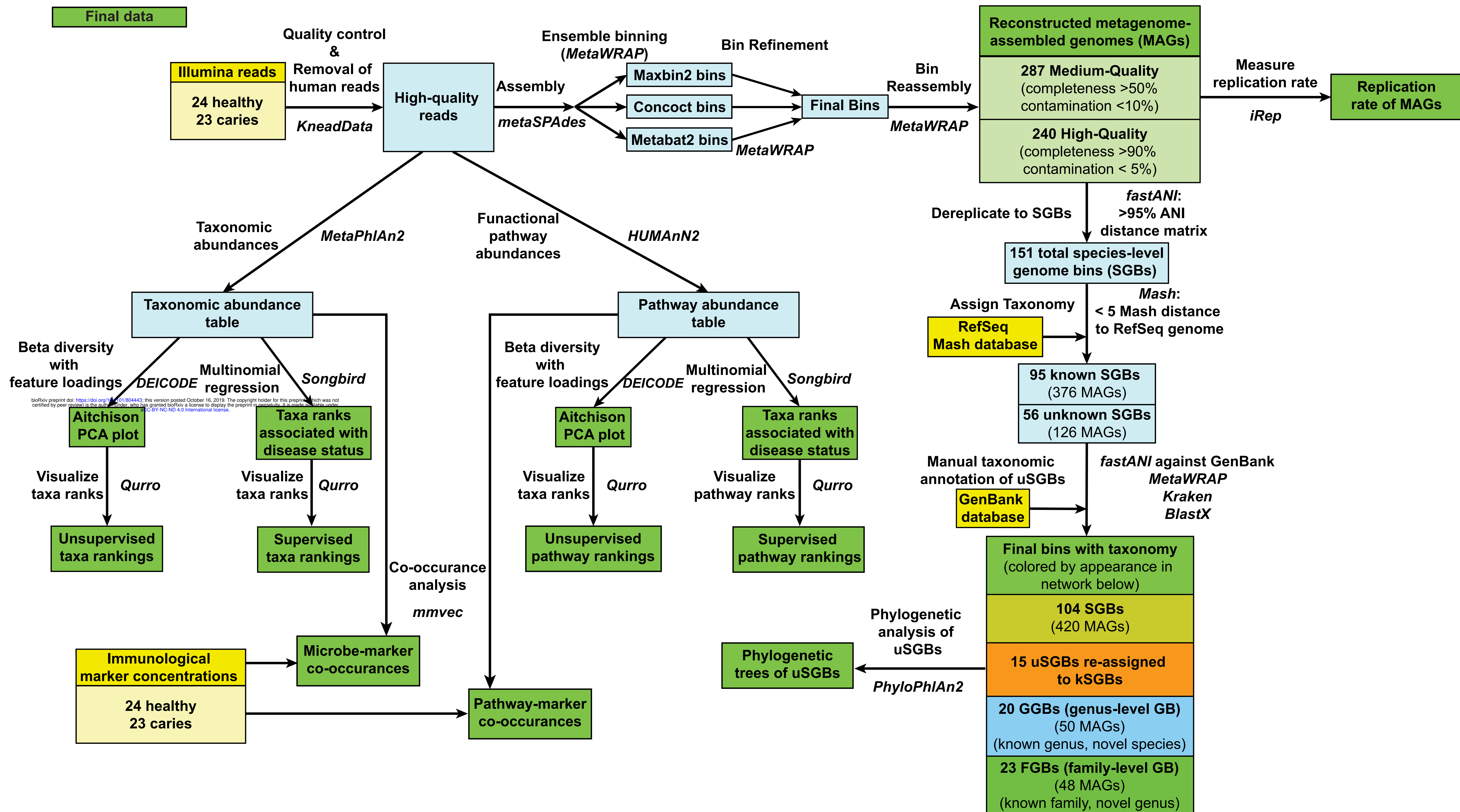
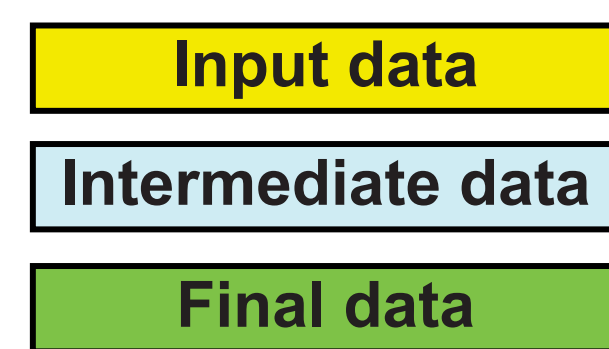
Figure 1**Summary of study design****A****B****Bioinformatics/Metagenomics Pipeline**

Figure 2

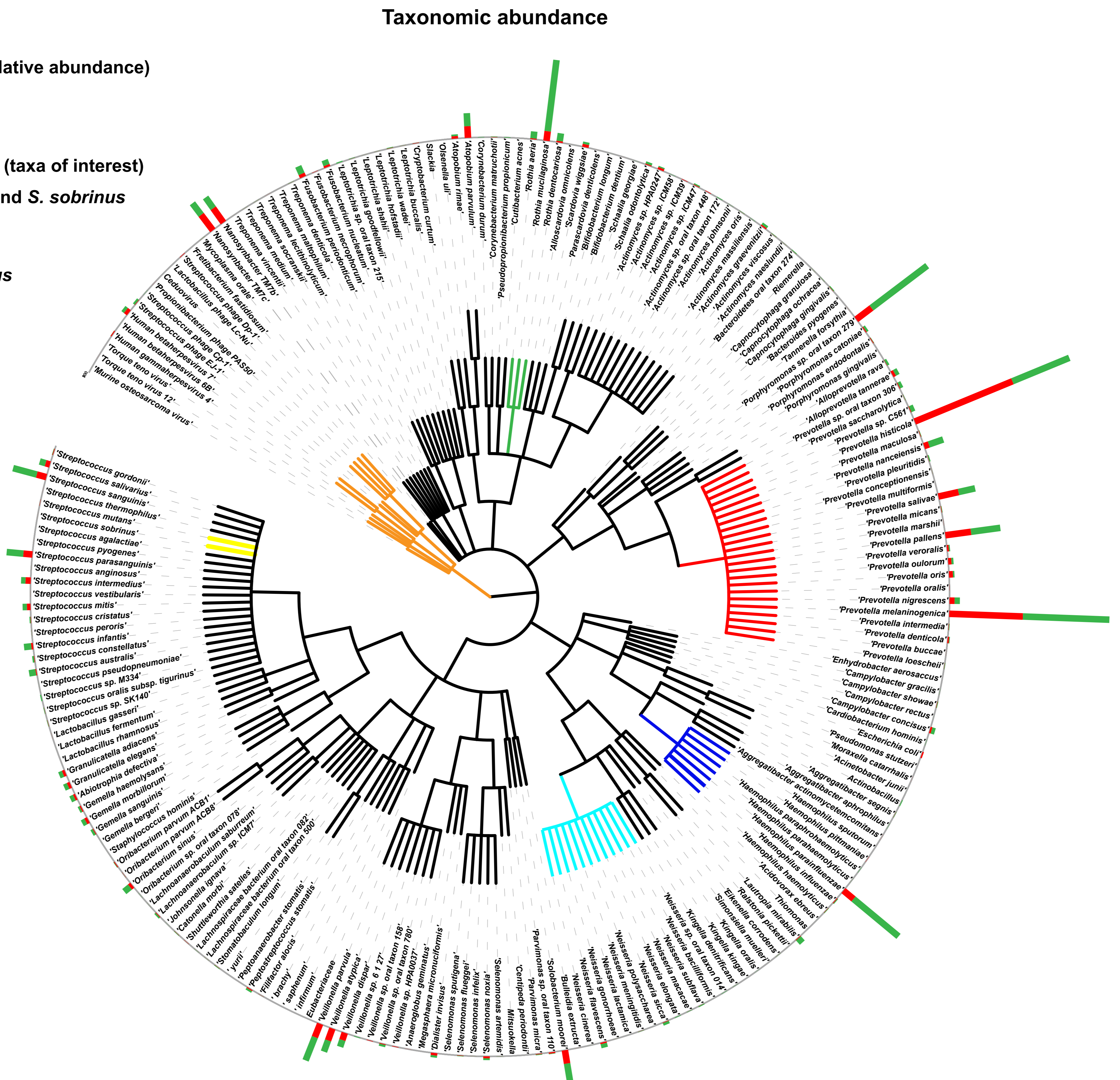
A

Bar graphs (relative abundance)

- Caries
- Healthy

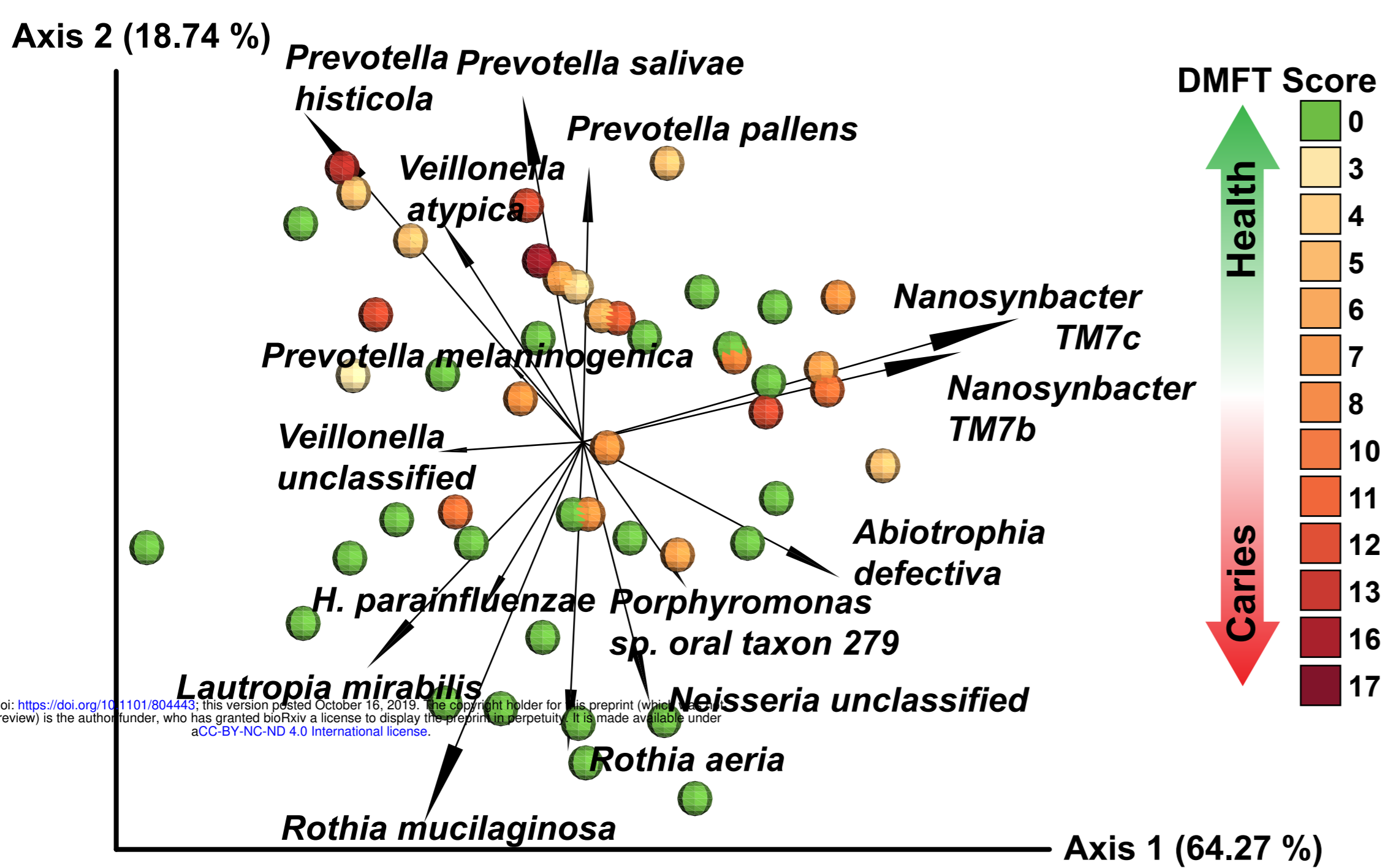
Tree Branches (taxa of interest)

- *S. mutans* and *S. sobrinus*
- *Prevotella*
- *Rothia*
- *Haemophilus*
- *Neisseria*
- Viruses



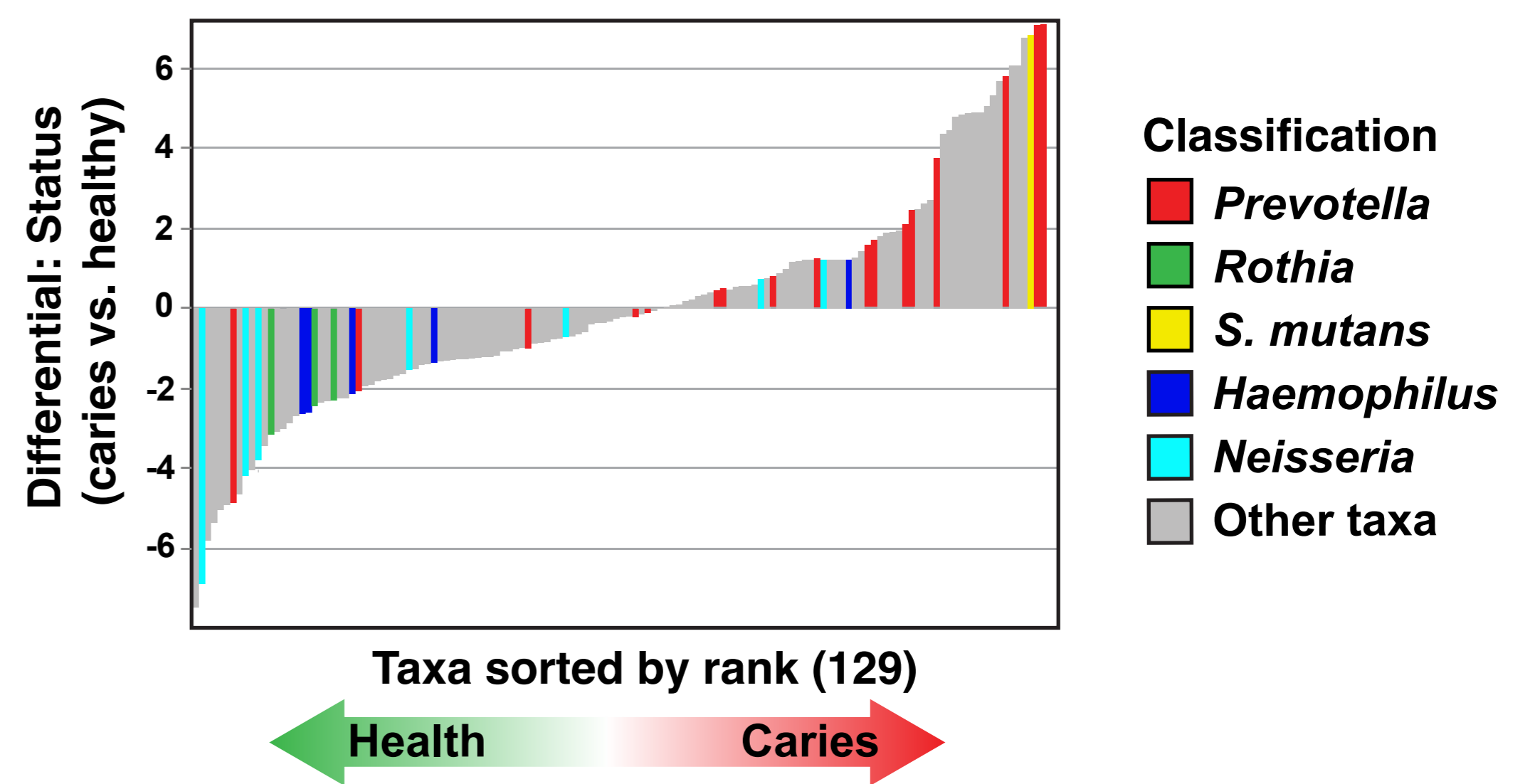
B

Aitchison PCA (beta diversity) with taxa loadings



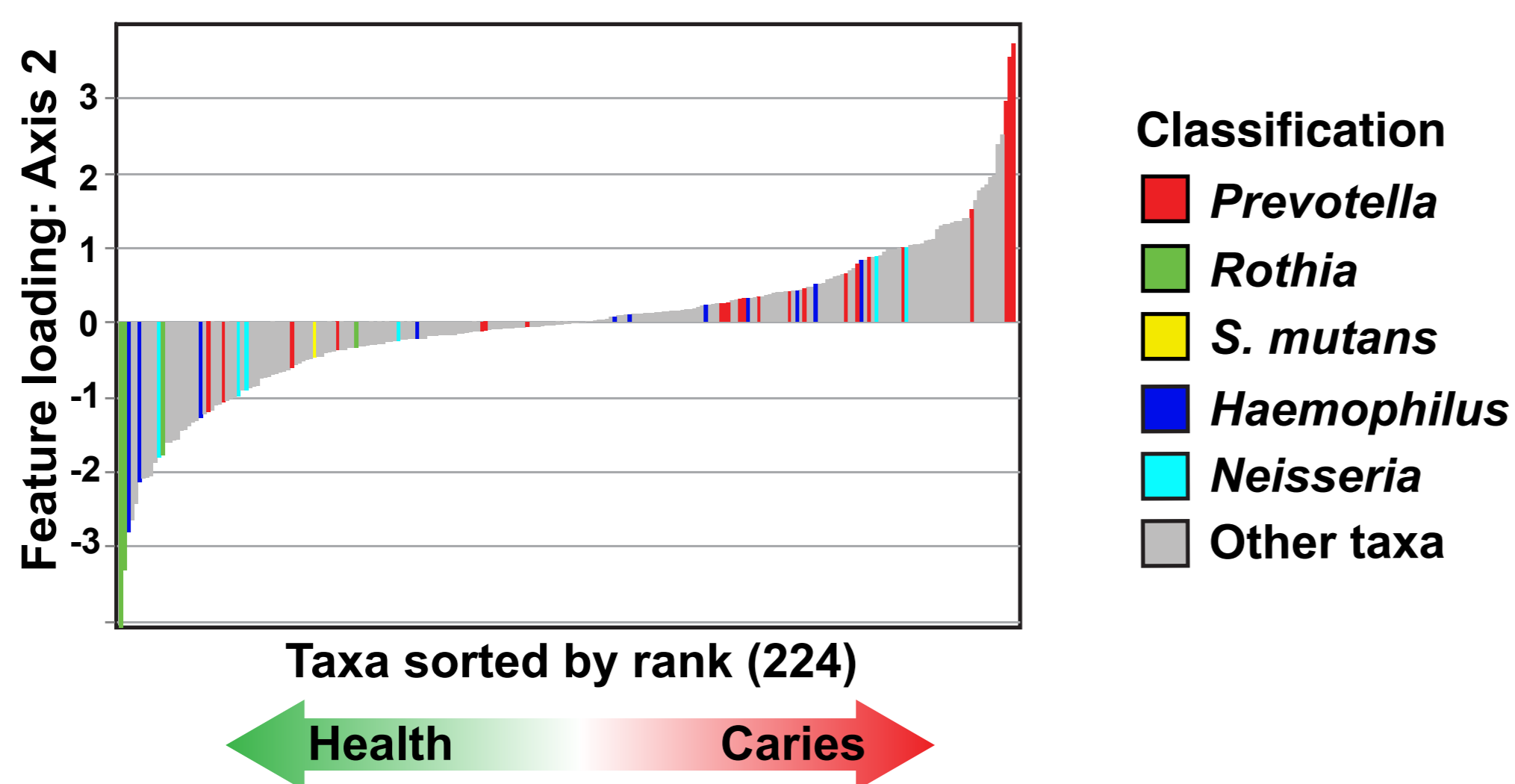
D

Taxa Associated with Caries vs. Health



C

Taxa driving distances in Axis 2 above



E

Prevotella/Rothia log-ratio

Prevotella/Haemophilus log-ratio

Prevotella/Neisseria log-ratio

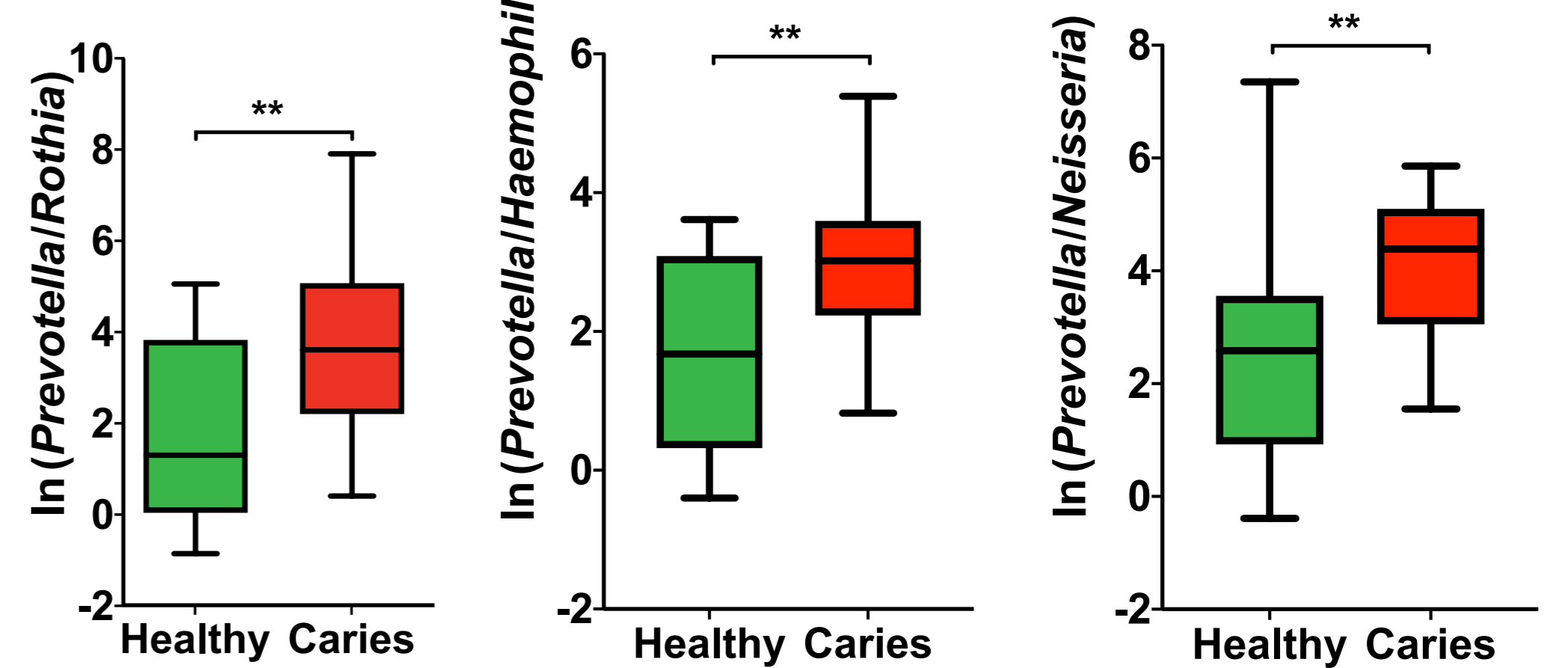
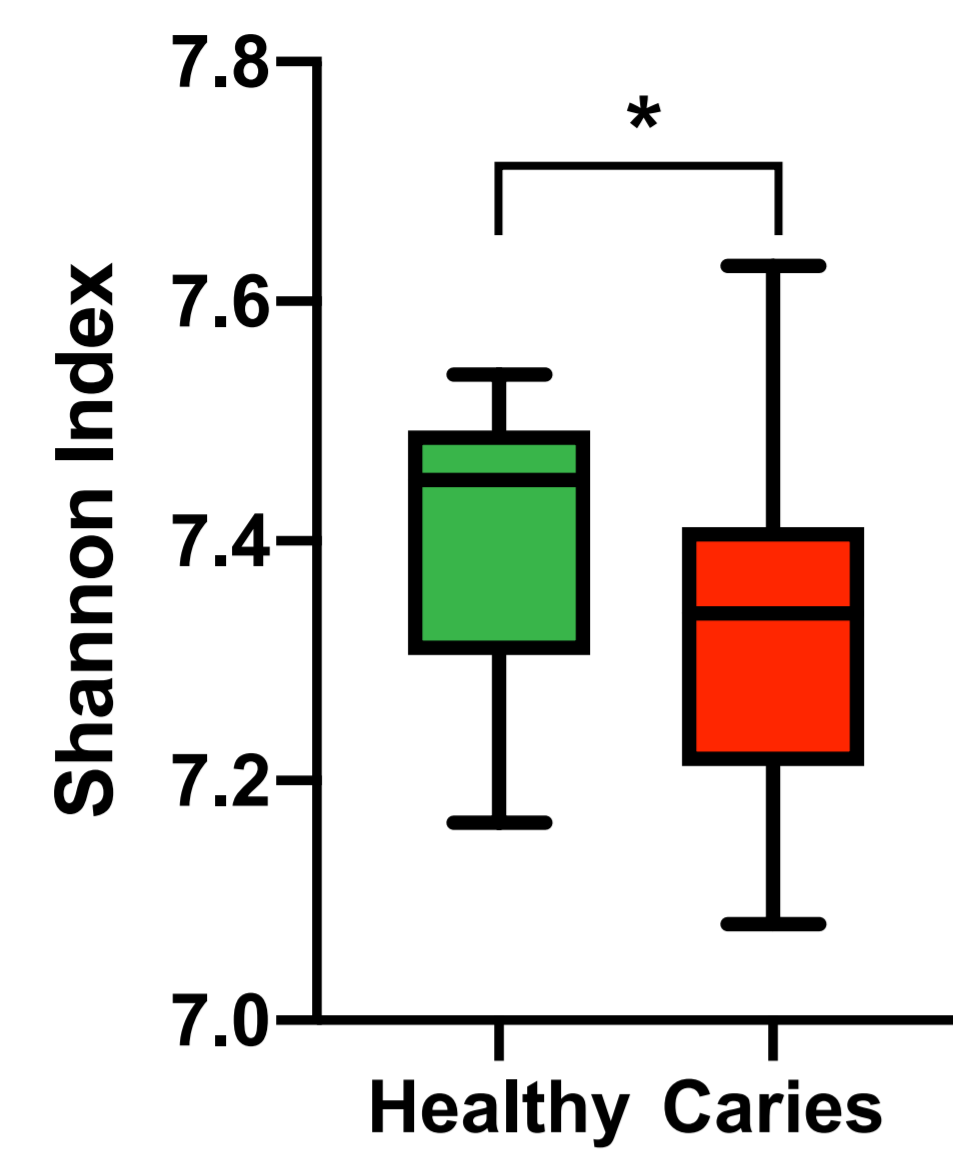


Figure 3

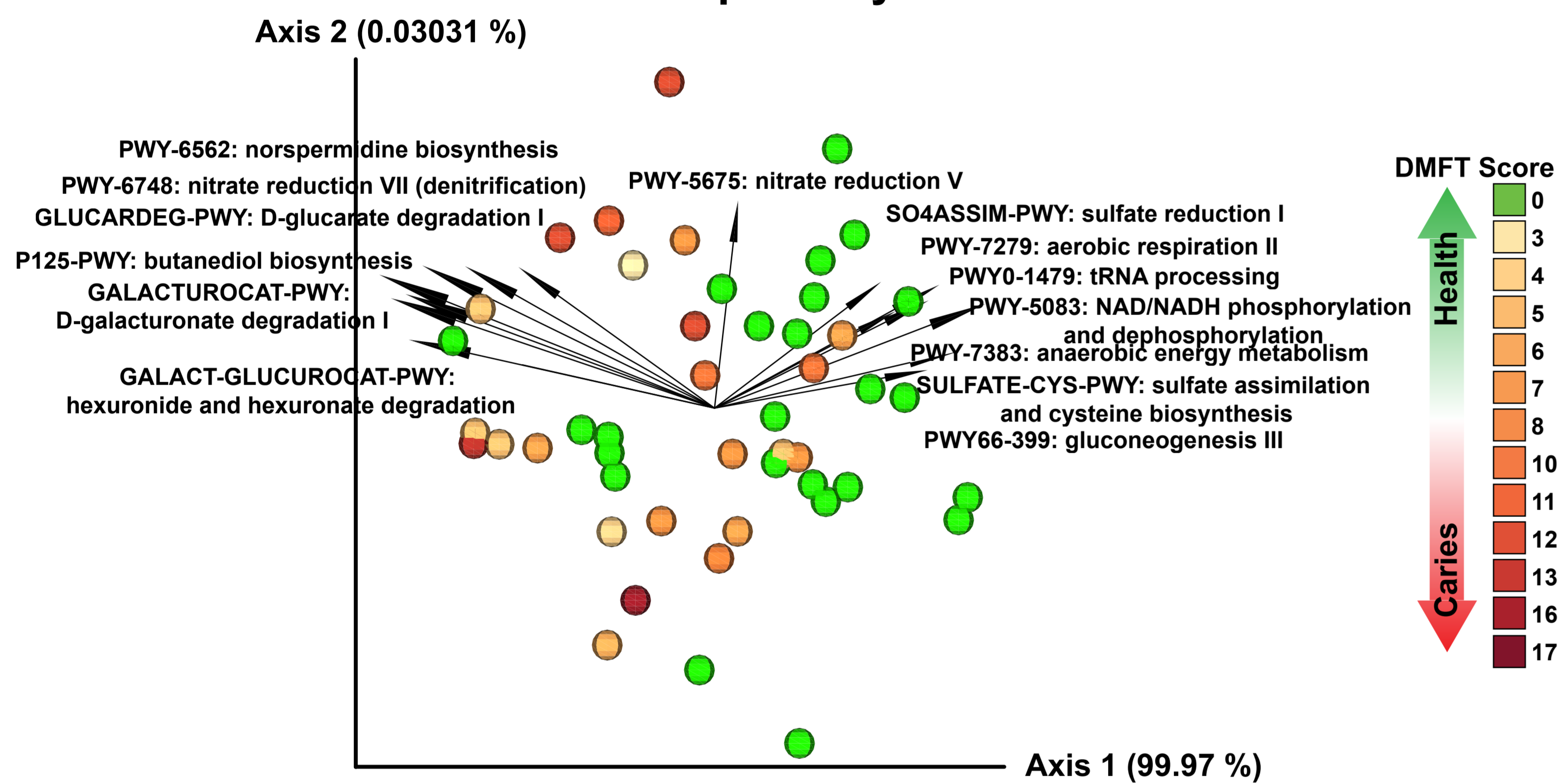
A.

Alpha diversity of functional pathways



B.

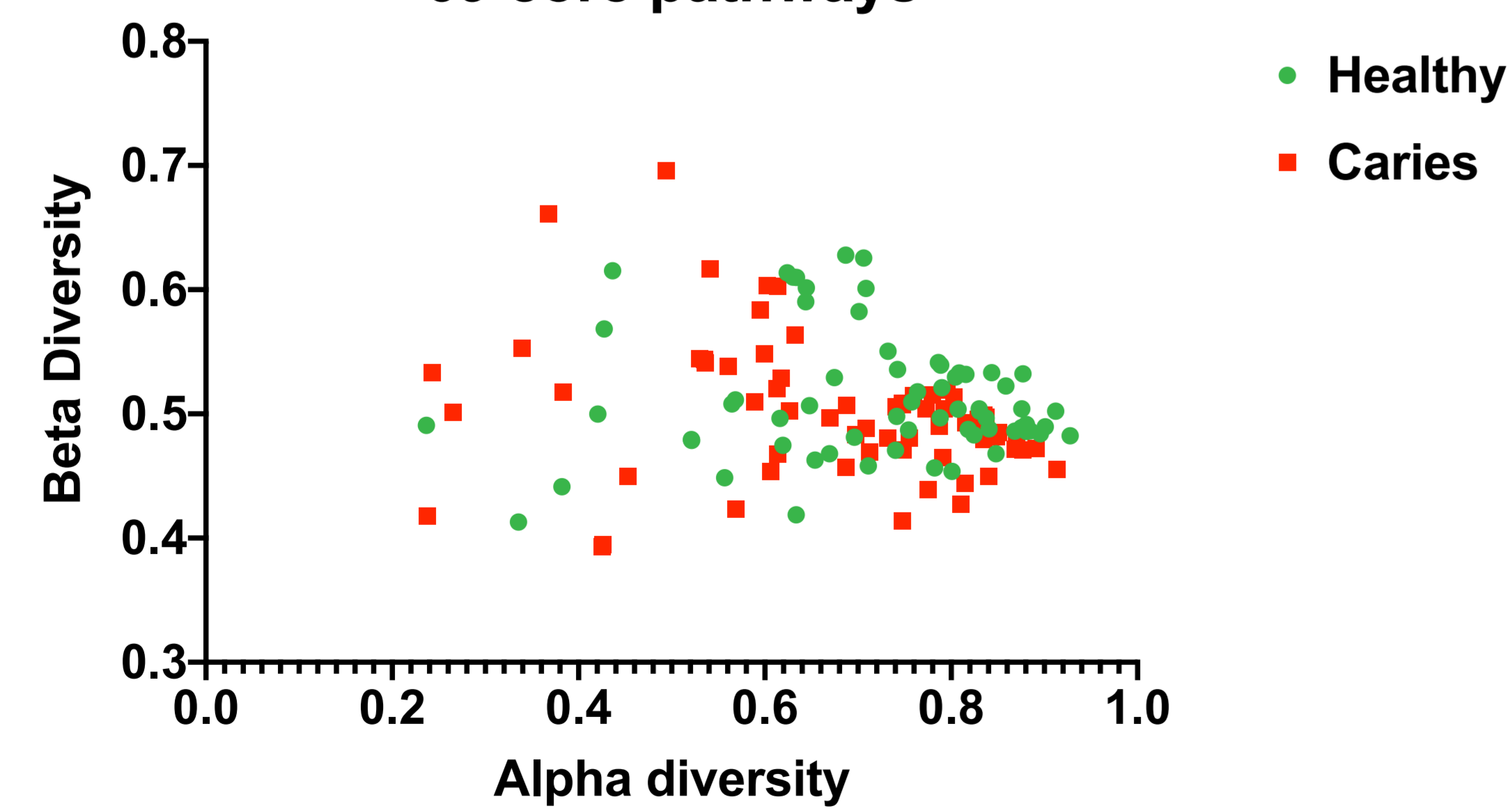
Beta diversity of functional pathways



C.

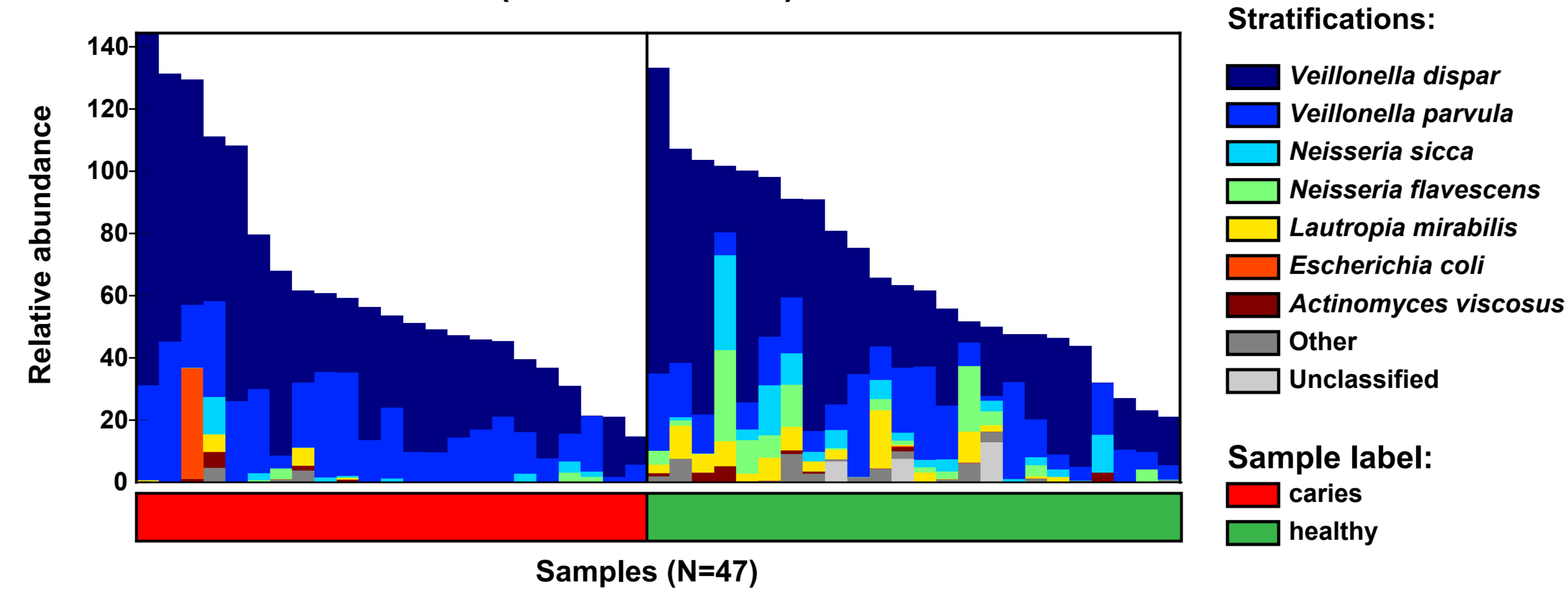
Contributrial Diversity

69 core pathways



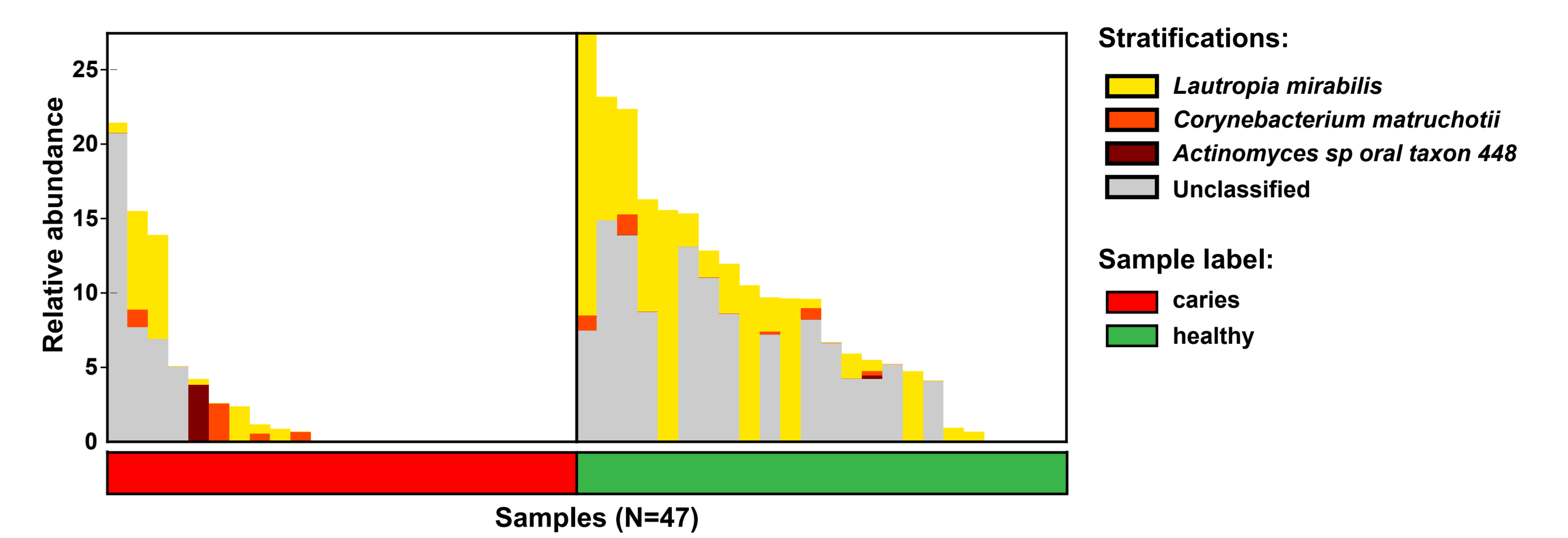
D.

Contributrial diversity: ARGSYN-PWY: L-arginine biosynthesis I (via L-ornithine)



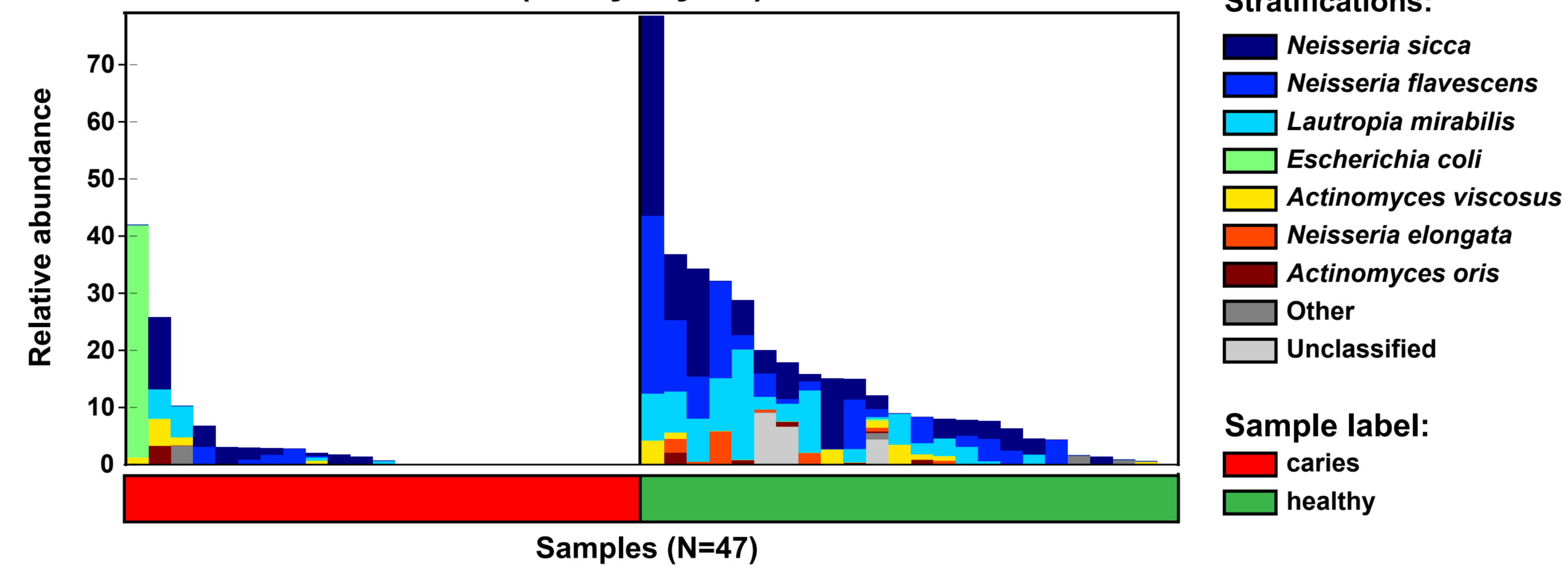
H.

Contributrial diversity: PWY-7383: anaerobic energy metabolism



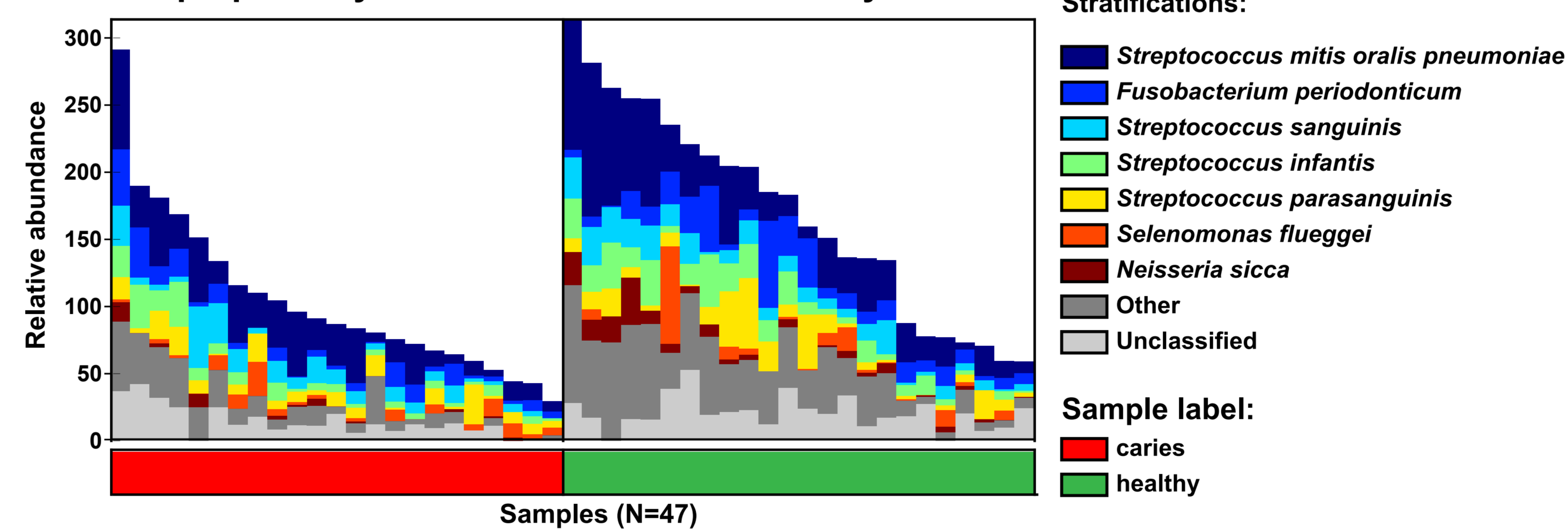
E.

Contributrial diversity: ARGSYNBSUB-PWY: L-arginine biosynthesis II (acetyl cycle)



F.

Contributrial diversity: BRANCHED-CHAIN-AA-SYN-PWY: superpathway of branched amino acid biosynthesis



G.

Contributrial diversity: PWY-7279: aerobic respiration II

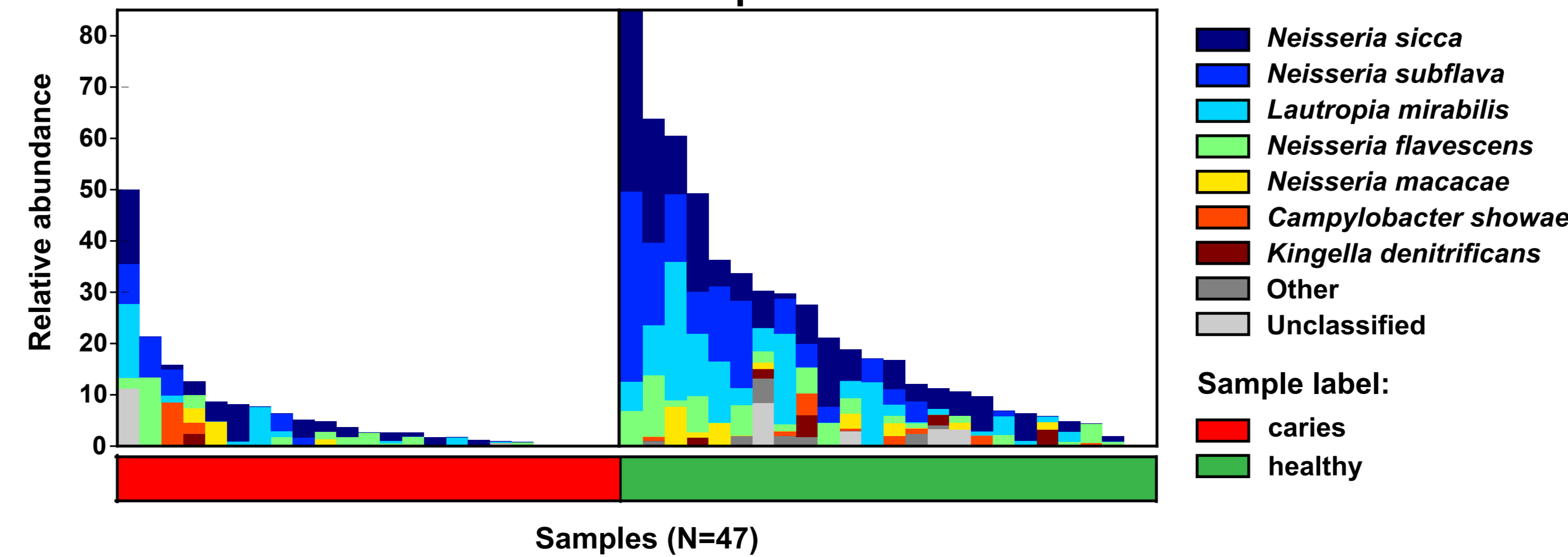
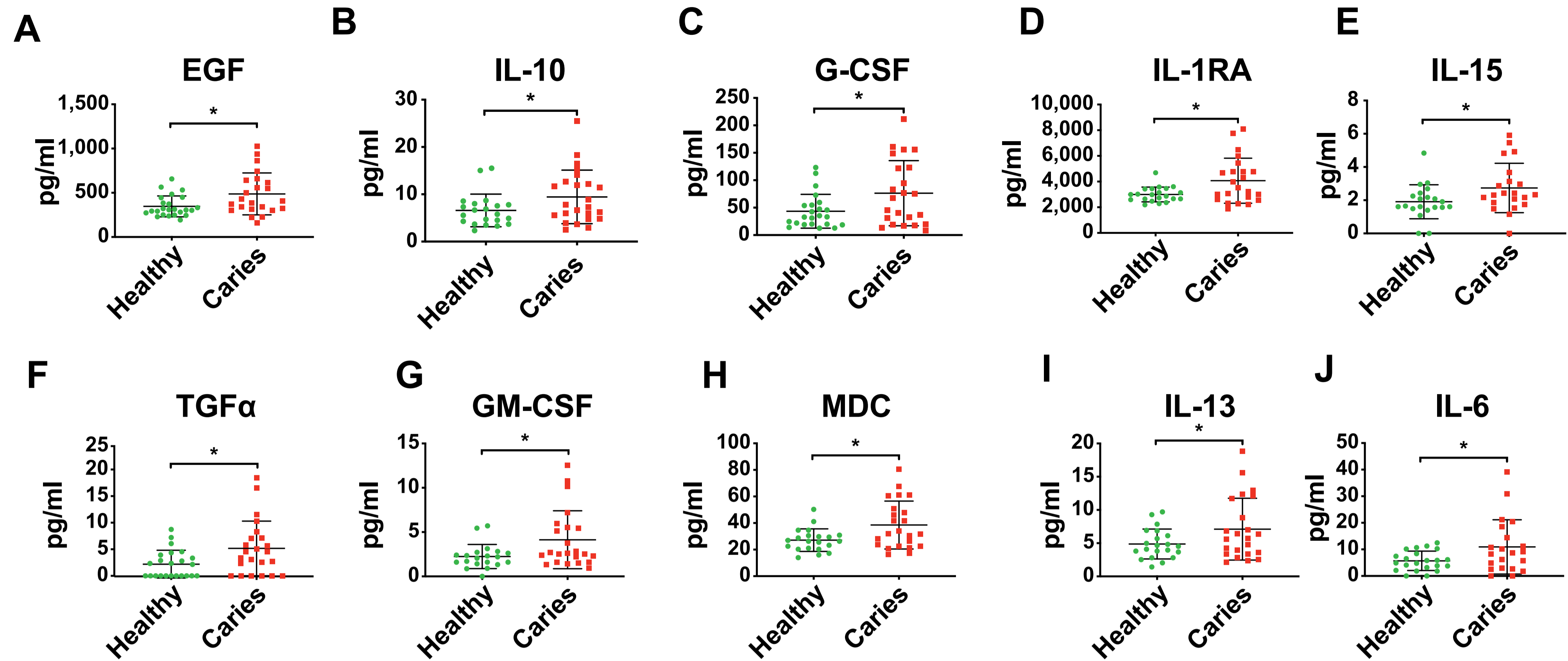
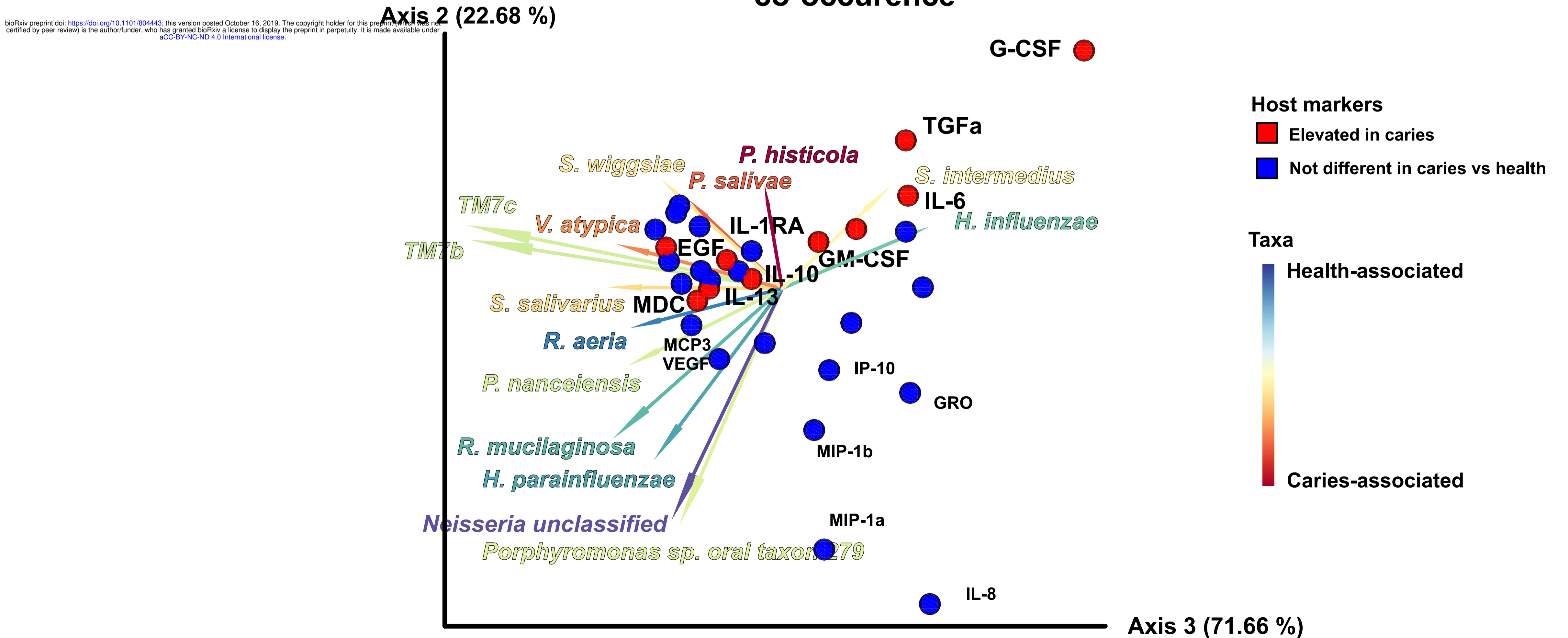


Figure 4

Salivary Immunological Markers



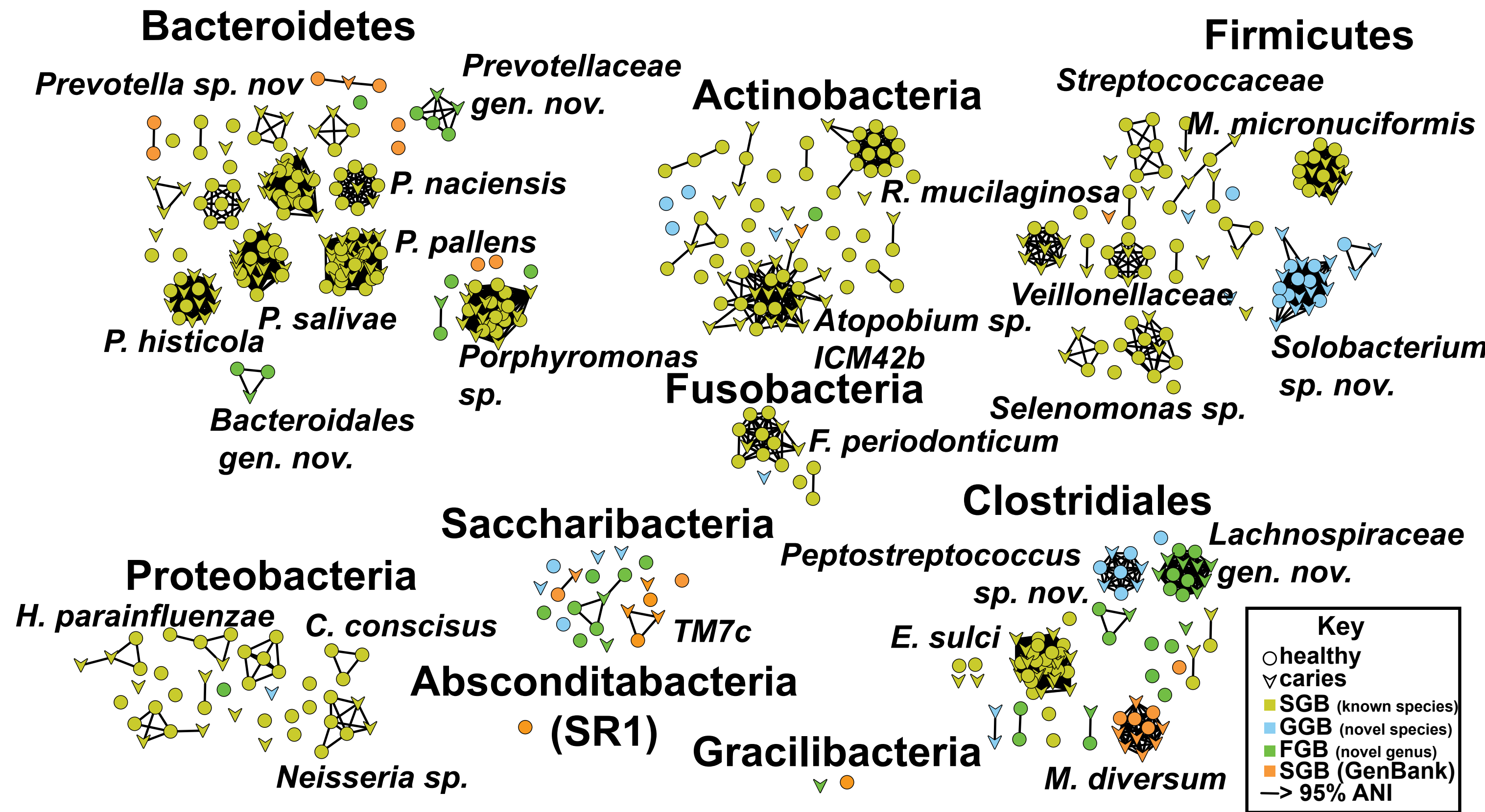
K Microbe-immunological marker co-occurrence



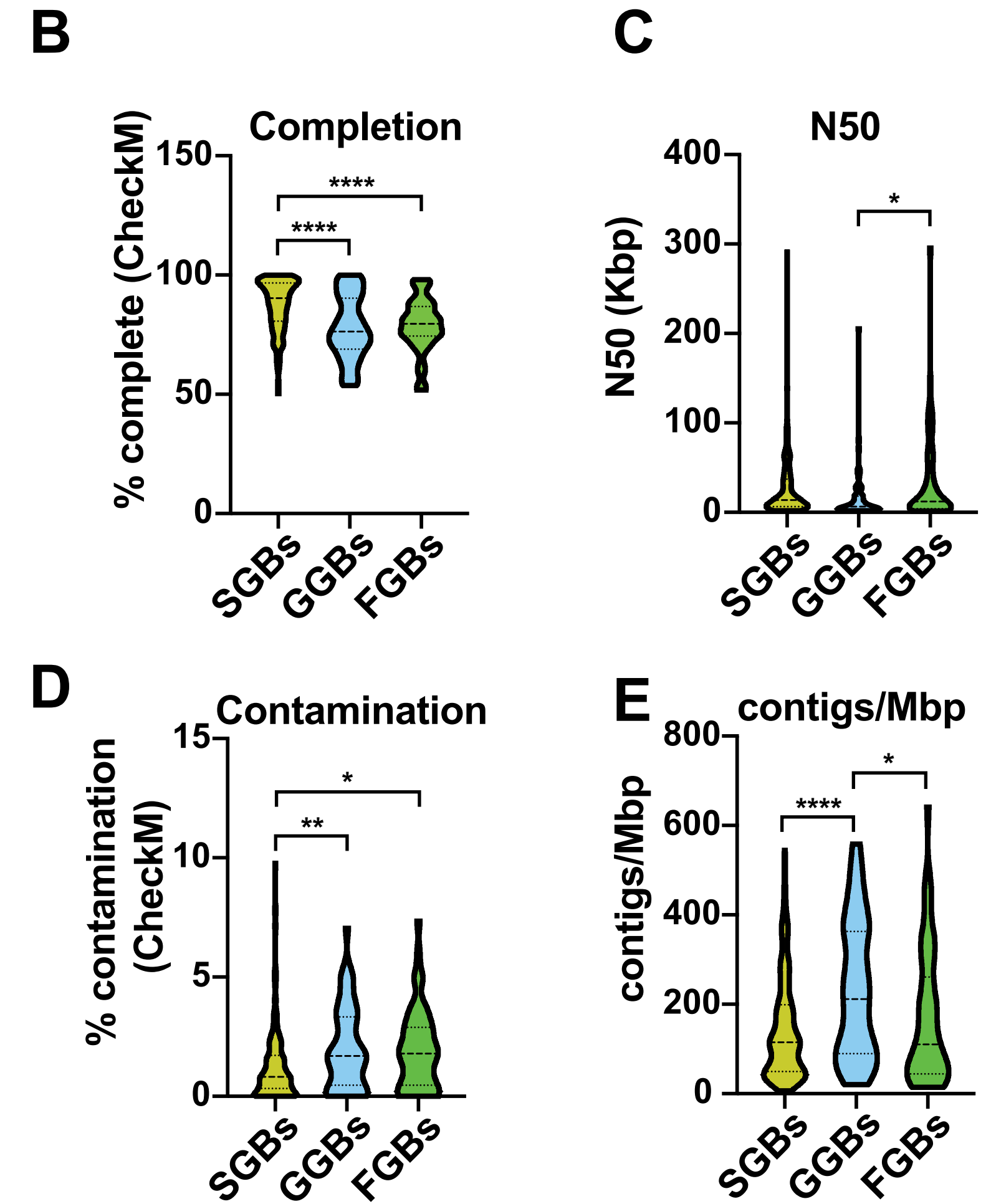
bioRxiv preprint doi: <https://doi.org/10.1101/804443>; this version posted October 16, 2019. The copyright holder for this preprint (which was not certified by peer review) is the author/funder, who has granted bioRxiv a license to display the preprint in perpetuity. It is made available under aCC-BY-NC-ND 4.0 International license.

Figure 5

A Recovered Genomes (MAGs)



MAG quality statistics



bioRxiv preprint doi: <https://doi.org/10.1101/804443>; this version posted October 16, 2019. The copyright holder for this preprint (which was not certified by peer review) is the author/funder, who has granted bioRxiv a license to display the preprint in perpetuity. It is made available under aCC-BY-NC-ND 4.0 International license.

Phylogenetic placement of major families of GGBs and FGBs (uSGBs)

